Evaluation of Iron Corrosion Release Models for Water Distribution Systems

Andrew Shea Benson

Thesis submitted to the faculty of the Virginia Polytechnic Institute and State University
in partial fulfillment of the requirements for the degree of

Master of Science
In
Environmental Sciences & Engineering

Dr. Andrea M. Dietrich, Chair
Dr. Daniel L. Gallagher, Member
Dr. Marc A. Edwards, Member

April 23, 2009
Blacksburg, VA

Keywords: Red Water, Iron Corrosion, Water Distribution, Modeling

Evaluation of Iron Corrosion Release Models for Water Distribution Systems

Andrew Shea Benson

ABSTRACT

Customer complaints of red water problems remain to be a frequent occurrence for water utilities. While material sources may vary, it is generally accepted that iron rust resulting from corrosion of iron based pipes is the predominant cause of red water issues. Recent efforts have lead to the development of a number of models that predict the occurrence of iron release and subsequent red water formation. This paper provides a detailed analysis of recently developed iron corrosion release models. Significant disagreement exists as to the processes and mechanisms leading to the release of iron corrosion materials into the water supply. This lack of consensus is made evident when comparing each of the iron release models. Considerable variation exists as to mechanisms considered and specific modeling goals. While each model may be beneficial for simulating certain aspects of corrosion release, no single model has been developed that provides a comprehensive portrayal of iron corrosion release phenomena.

TABLE OF CONTENTS

LIST OF FIGURES

LIST OF TABLES

1. BACKGROUND

Red water is one of the most prominent causes of consumer complaints and aesthetic water quality problems affecting water utilities. Red water is typically associated with concentrations of iron in the bulk water. Iron may be derived from source water, treatment processes, or most likely from iron pipe corrosion (Sarin, Snoeyink et al. 2001; Sarin, Snoeyink et al. 2004; Seth, Bachmann et al. 2004; Boxall and Saul 2005; Mutoti, Dietz et al. 2007a; Husband, Boxall et al. 2008).

Iron corrosion in water distribution systems (WDS) is an extremely complex electrochemical/ physicochemical process that results from chemistry at the interface between the water and the pipe wall as well as the physical/ mechanical characteristics of flow through the pipe. Corrosion results in the deterioration of metal (iron) pipe by an oxidation reaction at the pipe surface. As a result of this reaction, scaling forms on the pipe wall. While corrosion scaling can aid in corrosion resistance in the WDS by creating a barrier between the conductive water and the metallic surface of the pipe, it also serves as a reservoir for corrosion products that can be released into the water supply. Thus, it is important to point out the distinction between the rate of corrosion and the release of corrosion scale products in the water supply. While the rate of corrosion influences how much material is available for release into the water supply, the mechanism of release is often unrelated. Primary corrosion processes are well understood for the most part being the subject of research efforts over the previous decades. On the other hand, the processes and mechanism(s) of corrosion scale release are not as thoroughly understood and some disagreement still exists among experts. Factors influencing the release of corrosion scale

materials are derived from a wide variety of issues associated with water chemistry, biological processes, composition of pipe scale, and the hydraulic flow characteristics within the pipe.

While release mechanisms remain the subject for research and debate, efforts to develop predictive models for iron scale release have come about of late. The incorporation of predictive modeling capabilities would be highly desirable for a number of reasons. Predictive models could be incorporated with existing commercially available water distribution modeling software packages to allow for quick simulation and visualization. The use of an accurate corrosion release model could greatly assist with efforts to minimize the occurrence of red water events as well as general operation and maintenance for existing networks. A comprehensive iron corrosion release model would ideally incorporate all aspects of corrosion rate, scale formation, and release. As mentioned above, each of these components are individually (and often independently) affected by water chemistry, biological processes, pipe material/pipe scale composition, and hydraulics. At this point, such a model is unrealistic due to the limitations of current understandings of the processes involved. Each of the models developed to date typically emphasize one or two mechanisms for predicting iron concentration in delivered water. This paper intends to identify, categorize, and evaluate these models.

This report begins with a background of iron corrosion in water distribution systems. Section 1.1 deals with the fundamentals of iron corrosion processes in distribution systems. A general background of corrosion causes and effects is included. Section 1.2 deals with passive corrosion scale formation processes and composition. A detailed description of typical iron corrosion scale layers is included. Section 1.3 is

intended to provide a discussion of current knowledge surrounding the factors that affect iron corrosion scale release. Hydraulic, biological, and chemistry related factors are included. Chapter two provides a short discussion of the effects of corrosion in iron water distribution networks. Aesthetic effects, health effects, and alterations to the pipe are included. Chapter three then provides a characterization of available corrosion release models. These include the the Resuspension Potential Method, the Particulate Sediment Model, the 2-D Transient Corrosion model, the Prediction of Discoloration in Distribution Systems model, the Statistical Red Water Release Model, and the Iron Release Flux Model. Chapter four then provides an evaluation of the various applications and limitations of each of these models.

1.1 Principles of Iron Corrosion in Drinking Water Distribution Systems

Corrosion in water distribution systems involves the electrochemical or physicochemical interaction between the pipe (usually metal) and the water traveling through the pipe. Two problems may arise from pipe corrosion; namely deterioration/failure of the water distribution network and unwanted alterations to water quality. An oxidation (electron transfer) reaction provides for the deterioration of the interior pipe surface providing there exists a difference in electrical potential at two different points on the pipe surface (AwwaRF and Wasser 1996). Four components are necessary for the propagation of this reaction:

- Anode: The anode is the location on the pipe surface where oxidation occurs. Electrons are released and transferred through the internal circuit (pipe wall) to the cathode. Positive metals ions are released upon oxidation of the anode.

- Internal Circuit: The internal circuit provides the pathway of electron transfer to the cathode. This corresponds to the pipe wall in water distribution lines.
- Cathode: The cathode is the location on the pipe surface where reduction occurs. Electrons accepted at the cathode combine with available dissolved oxygen and water to form negative ions (OH^-).
- External Circuit: The external circuit is an electrolyte solution allowing for conduction between the cathode to the anode. This corresponds to the water traveling through the pipe.

Figure 1 below shows a depiction of this process. Note that the acronym 'Fe' corresponds to the iron that makes up the pipe wall. Also, note that the formation of iron hydroxides (FeOH) and other compounds on the pipe wall corresponds to surface tuberculation. Dissolved oxygen is consumed on the cathodic side of the circuit to allow for hydroxide formation (increased pH).

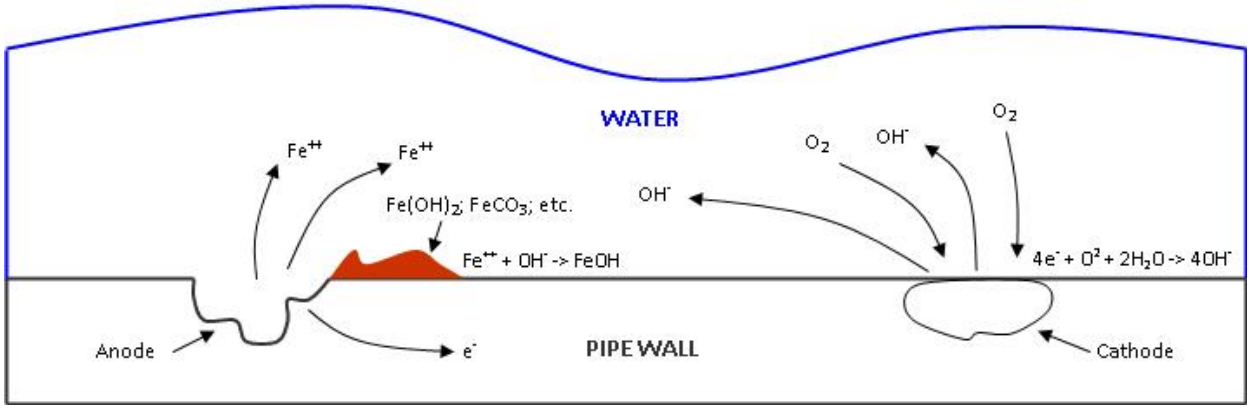

Figure 1 Diagram of iron corrosion cell reaction at pipe wall

Although useful, the depiction of corrosion in water distribution systems detailed in Figure 1 above is in many ways an oversimplification. There are a wide array of chemical

reactions that occur at the pipe surface that relate to corrosion and are specific to water quality and pipe characteristics. These interactions will be discussed further in later sections of this report.

1.1.1 TYPES OF CORROSION

Uniform Corrosion

Uniform corrosion occurs when there is equal rate of deterioration across an area of pipe surface. The result is even thinning of the pipe thickness and ultimately weakening of the structural integrity of the pipe. Uniform corrosion results from alterations between anodic and cathodic conditions at a single location on the pipe. At any time, a certain section of pipe could resemble either the anode or cathode. This variation of conditions over the various sections of the entire surface of the pipe allows for relatively even corrosion across the surface.

Localized Corrosion

Localized corrosion can result from imperfections in the pipe surface, areas of high stress, ruptures in the pipe coating, a difference in the concentration of aqueous species between two locations in the pipe, etc. There are four types of localized corrosion: galvanic, pitting, and crevice.

Galvanic

Galvanic corrosion occurs when two different metal pipes are in contact and the conditions of the corrosion cell are present. One metal acts as the anode, the other as the cathode, the connection between the two is the internal circuit, and water as the external circuit. In this circumstance, the anodic and cathodic locations are fixed in do not vary as such with uniform corrosion. This type of corrosion is exemplified by increased

deterioration close to the junction of two dissimilar pipes. Figure 2 below reveals groupings of metals that tend to be anodic/more corrosive and cathodic/less corrosive. A metal on the left connected to a metal on the right of this series will tend to act as the anode. The greater the distance between the two metals indicates a greater potential difference. Other factors such as water quality and temperature may influence the position of the metal on the series though (under certain conditions, iron may be anodic to zinc) (AwwaRF and Wasser 1996). This type of corrosion can be avoided by the use of non-conducting insulators placed between the dissimilar pipes.

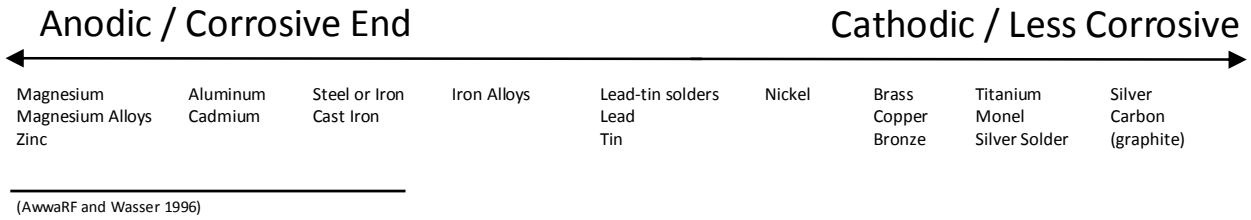

(AwwaRF and Wasser 1996)

Figure 2 Galvanic corrosion series of metals

Pitting

Pitting is a general term used to describe a class of localized corrosion. Pitting can be one of the most destructive forms of corrosion as the indentations on the pipe wall create pinholes resulting in ruptures in the pipe. Pits arise from a tiny region of pipe resembling anodic conditions over an extended period of time. The result is a small but steep depression or pit. Once a pit is formed, continued corrosion occurs as the pit creates the conditions necessary for further corrosion. Specific causes of pitting corrosion vary from imperfections in the metal or scale, regions of high stress in the metal, or a difference in concentration of aqueous species at two locations in the pipe. The rate of corrosion depends on the type of pipe and water quality characteristics.

Crevice

Crevice corrosion results from small areas of isolated or otherwise shielded locations on the pipe surface. Water in these crevices may have a different makeup than the bulk water traveling through the pipe causing a potential difference between the two locations. Changes in water characteristics may also heighten this form of corrosion by exaggerating differences between crevice water and bulk water. Possible sites of crevice corrosion include holes, gasket surfaces, pipe joints, surface deposits, and corrosion products (Kirmeyer and Logsdon 1983).

Concentration Cell Corrosion

Variation in concentration of certain aqueous species within a WDS can also drive corrosion processes. Such species include dissolved oxygen and hydrogen ion (H^+). Causes for variation in aqueous concentration may include localized corrosion processes, reaction of oxygen with corrosion products, microbial conditions, scaling that prevents diffusion of oxygen to pipe surface, etc. The corrosion reaction always moves towards equilibrium and thus will always tend to equalize the potential between regions. Since oxygen is utilized in the cathodic reaction, area of high DO concentration end up as cathodic sites and areas of decreased DO concentration act as the anode. If conditions allow for continued maintenance of differential concentration, the corrosion reaction will be also be maintained potentially causing significant deterioration. (AwwaRF and Wasser 1996)

Biologically Enhanced Corrosion

There are two main processes by which microbes can enhance corrosion processes in the WDS. First, the growth of microbes on the pipe surface can create regions of differing dissolved oxygen, hydrogen ion, and metal ion concentrations. This leads to localized concentration cell corrosion. Additionally, microbes may be responsible for

oxidation/reduction reactions that directly affect corrosion processes. Microorganisms have been discovered in water distribution systems that convert Fe(II) to Fe(III), Fe(III) to Fe(II), sulfate to sulfite, sulfite to thiosulfite, thiosulfite to sulfide, sulfite to sulfate, as well as organisms responsible for nitrosofication, nitrification, and denitrification. These reactions may either directly or indirectly affect both corrosion reactions and corrosion scale formation. (AwwaRF and Wasser 1996)

Morton and others discussed the role of corrosion in aiding bacterial growth in the WDS. Iron/steel based pipes used in WDS may contain up to 0.2% phosphorous by weight as a result of the manufacturing process. Phosphorous is a known limiting nutrient associated with microbial growth. This work showed that as iron/steel pipe corrodes, forms of phosphorous are released into the pipe environment. The levels of phosphorous released were found to be sufficient to support bacterial growth. Further, corroding iron/steel can abiotocally produce all the principle nutrients necessary for bacterial growth (Morton, Zhang et al. 2005). Other studies have shown that the addition of corrosion inhibitors (orthophosphates and sodium silicates) had no significant impact on biofilm growth. Growth of biofilms in the WDS were found to be independent of the concentration of orthophosphate in the bulk water (Rompre, Prevost et al. 1999). This implicates the role of corrosion in assisting bacterial growth as opposed to the availability of phosphorous in finished drinking water.

1.1.2 PIPE MATERIAL AND CORROSION

Water distribution networks typically include a wide variety of pipe materials depending on the date of installation, local conditions, etc. Pipe materials may include unlined cast iron, lined cast iron, ductile iron, galvanized, copper, lead, polyvinyl chloride

(PVC), polyethylene, or others. Additionally, it is possible that a protective liner has been added to aged pipe. Ultimately, the corrosive properties of a pipe relate to the material that interfaces with the water in the pipe. For example, an iron pipe that has a concrete liner will exhibit corrosive behaviors similar to a concrete pipe. To complicate the matter, protective liners frequently deteriorate with time and expose the interior surface of the pipe. While corrosive behaviors of specific materials may be characterized, the actual conditions within an aged water distribution network may be unknown. Regardless, as this report is primarily concerned with iron corrosion, the corrosive properties of iron based pipes (unlined cast iron and galvanized pipe) are solely characterized.

1.1.3 CORROSION INDICES

A variety of efforts have been undertaken to provide and simple and easy to use indicator for the corrosivity of treated water. Many of these indices provide an indication as to a water's capability of precipitating calcium carbonate ($CaCO_{3(s)}$). Precipitated calcium carbonate (or calcite) is thought to provide a protective 'eggshell' layer along the surface of pipes that prevent the corrosion reaction from proceeding. Such indices include: the Langelier Saturation Index, the Ryznar Index, the Aggressiveness Index, the Driving Force Index, Dye's Momentary Excess, and the Calcium Carbonate Precipitation Potential (McNeill and Edwards 2001). Other indices developed attempt to incorporate other water quality variables and their implications on corrosion of distribution network pipes. These include the Larson Ratio, the Modified Larson Ratio, and the Riddick Corrosion Index (Imran, Dietz et al. 2005). Regardless of their widespread use though, no single index has been found to be the cure all end all for water corrosivity. This is likely due to the shear complexity of corrosion interactions. There are over 15 water quality parameters that are

thought to have some effect on corrosion. Differentiation must also be made between the corrosion reaction, scale formation processes, and scale release/red water problems. Each water quality parameter may have varying effects on each of these processes. Thus, the use of any corrosion index should be approached with caution. A summary of corrosion indices and the water quality parameters used to calculate them can be found in Table 1 below. A more detailed summary of the Langelier Index, the Ryznar Index, and the Larson Ratio follow.

Table 1 Summary of parameters necessary to calculate corrosion indices

	Corrosion Index							
Parameter	LI	RI	CCPP	RCI	DFI	AI	LR	LRM
pH	X	X				X		
Alkalinity			X	X		X		X
CO_2 ; $H_2CO_3^o$				X				
HCO_3^-	X	X					X	
CO_3^{2-}					X			
Ca^{2+}	X	X	X		X			
SO_4^{2-}							X	X
Cl^-				X			X	X
NO_3^-				X				
Hardness				X		X		
SiO_2				X				
DO				X				
Sat. DO				X				
Na^+								X
Temp								X
HRT								X

NOTE: Ionic strength is required when effects of activity are considered for dissolved species.

LI = Langelier Index; RI = Ryznar Index; CCPP = Calcium Carbonate Precipitation Potential; RCI = Riddick Corrosion Index; DFI = Driving Force Index; AI = Aggresiveness Index; LR = Larson Ratio; LRM = Modified Larson Ratio

(Imran, Dietz et al. 2005)

Langelier Index

The Langelier Index (LI) is a measure of a water's pH relative to its pH of saturation with $CaCO_{3(s)}$. Essentially, the LI provides an indication as to whether a water will precipitate $CaCO_{3(s)}$ or if it is undersaturated with respect to Calcium ($Ca^{2+}_{(aq)}$) and Bicarbonate ($HCO_3^-{}_{(aq)}$). The LI is derived from thermodynamic data for the following reaction:(Imran, Dietz et al. 2005)

$Ca^{2+} + HCO_3^- = CaCO_{3(s)} + H^+$; $K_{sp} = 10^{-1.85}$

LI is determined from the following equation:

$$LI = pH_a - pH_s$$

Where:

$pH_s = pK - \log[Ca^{2+}] - \log[HCO_3^-] - \log \gamma_{Ca^{2+}} - \log \gamma_{HCO_3^-}$ (AwwaRF and Wasser 1996)

In which:

LI = Langelier Index

pH_a = measured pH

pH_s = pH at which solution is saturated with $CaCO_{3(s)}$

pK = 1.85 (Langmuir 1997) = -logK (K is the equilibrium constant for the above reaction)

$[Ca^{2+}]$ = Calcium ion concentration in Moles/Liter

$[HCO_3^-]$ = Bicarbonate concentration in Moles/Liter

γ = activity coefficient

A positive LI value indicates that water is saturated with respect to $CaCO_3$ and is thus deemed 'noncorrosive'. A protective layer of $CaCO_3$ is expected to form on the pipe wall. A negative LI value indicates that the water is undersaturated with respect to $CaCO_3$.

Concentration of Ca^{2+} can be measured using an electrode or can be determined in the lab via atomic absorption spectroscopy. Bicarbonate (HCO_3^-) concentration is related to alkalinity and for pH ranges of treated water (~6.5 – 9) can be assumed to equal alkalinity.[1]

Ryznar Index

The Ryznar Index is similar to the Langelier Index as it uses a waters tendency to precipitate $CaCO_3$ as an indicator for corrosivity. The pH_s term used in the Ryznar index calculation is identical to the pH_s term used to calculate the Langelier Index. The Ryznar Index is calculated as follows:

$$RI = 2*pH_s - pH_a$$

Where,

RI = Ryznar Index

pH_s = pH at which solution is saturated with $CaCO_{3(s)}$

pH_a = measured pH

Typically, an RI value between 5.0 and 7.0 is desireable. Heavy scale is expected to form when the RI is below 5.0 to 5.5. Significant corrosion is expected when the value is above 7.0. An increasing value for RI indicates and increasing corrosivity of a water.

Larson Ratio

The Larson Ratio (LR) incorporates the effects of chloride, sulfate, and bicarbonate concentration on the corrosivity of a water. The LR assumes that chloride and sulfate behave to enhance corrosion and that bicarbonate mitigates corrosion. The LR can be calculated as follows:

---

[1] Bicarbonate is the dominant alkalinity species for a pH range of ~ 6.5-9. Additionally, alkalinity is typically reported as mg/L as $CaCO_3$; to convert to Moles/L of bicarbonate, divide alkalinity by 5×10^4.

$$LR = \frac{(2*[SO_4^{2-}]+[Cl^-])}{[HCO_3^-]}$$

where [ ] is expressed in moles per liter. Values above 0.5 are considered to be corrosive. A recent study attempted to modify the LR to incorporate the additional effects of temperature, sodium, and hydraulic retention time (Imran, Dietz et al. 2005). Results from a two year pilot study have provided results superior to the LR. The new index is termed the Modified Larson Ratio (LRM) and is calculated as follows:

$$LRM = \frac{(Cl^-+SO_4^{2-}+Na^+)^{1/2}}{Alk}\left(\frac{T}{25}\right)HRT$$

Where chemical species are measured in mg/L, alkalinity is measured as mg/L $CaCO_3$, temperature is in units of degrees Celsius, and hydraulic retention time (HRT) is measured in days.

1.1.4 Monitoring Corrosion and Corrosivity

There are a wide variety of instruments available to monitor corrosion in water distribution systems. These monitors can be incorporated into existing SCADA systems. Typically, these instruments utilize a sacrificial piece of metal that is inserted into the WDS and the electrical resistance across the metal is measured. While useful for identifying the corrosiveness of the water in relation to the piece of metal, correlating this measurement to the corrosive activity in the WDS proves complicated. As mentioned previously, the rate of corrosion of a pipe surface bears no simple relationship to the release of iron scale materials. Additionally, in aged networks, delivered water interfaces with passive scale and not the clean metal pipe surface. Measuring electrical resistance along a sacrificial metal will not necessarily correspond to corrosion processes that involve layers of scale. Another difficulty arises when considering the variability in water quality throughout the

WDS. Corrosion monitors located sparsely throughout the distribution system will only be able to provide an indication of corrosivity at discrete locations.

1.2 Iron Corrosion Scale Formation and Composition

Scale formation processes and transformations are extremely complex incorporating a variety of oxidation – reduction, dissolution – precipitation, and acid – base reactions between the pipe surface, corrosion scale layers, and the specific chemistry of the water in the pipe (as well as microbes that may exist within the scale). While a variety of thermodynamic equilibria govern reaction pathways, reaction kinetics, which may be greatly affected by water chemistry, also plays a large role in determining ultimate scale composition. Essentially, scale formation processes are associated with the fate and transformation of oxidized ferrous iron (Fe(II)) and the following changes that occur to iron scale as it ages. Table 2 below lists some of the reactions associated with iron corrosion and subsequent scale formation. Additionally, Table 3 lists other iron solids that may be found in corrosion scale layers.

Table 2 Reactions associated with iron corrosion

Reaction	Oxidation State of Fe Products	Description	Likley Location of Reaction
$Fe_{(s)} \rightarrow Fe^{2+} + 2e^-$	II	Oxidation of metallic iron	Pipe surface
$Fe^{2+} \rightarrow Fe^{3+} + e^-$	III	Oxidation of ferrous iron	Varies
$Fe^{2+} + 2OH^- \rightarrow Fe(OH)_{2(s)}$	II	Precipitation of ferrous hydroxide	Pipe surface, scale interior, scale surface layer, bulk water flow
$Fe^{3+} + 3OH^- \rightarrow Fe(OH)_{3(s)}$	III	Precipitation of amorphous ferric hydroxide	Scale interior
$2Fe^{2+} + 0.5O_2 + 4OH^- \rightarrow Fe_2O_3 \cdot H_2O + H_2O$	III	Oxidation of ferrous iron to form hematite (or maghemite)	Pipe surface
$3Fe(OH)_{2(s)} \rightarrow Fe_3O_{4(s)} + 2H_2O + 2H^+ + 2e^-$	II and III	Partial oxidation of ferrous hydroxide to form magnetite (FeO·Fe2O3)	Scale interior, scale surface layer
$Fe^{2+} + CO_3^{2-} \rightarrow FeCO_{3(s)}$	II	Precipitation of siderite	Scale interior
$3Fe^{2+} + 2PO_4^{3-} \rightarrow Fe_3(PO_4)_{2(s)}$	II	Precipitation of vivianite	Scale interior
$(1-x)Fe^{2+} + S^{2-} \rightarrow Fe_{(1-x)}S_{(s)}$	II	Precipitation of ferrous sulfide	Scale interior
$2Fe(OH)_{3(s)} \rightarrow \alpha\text{-}Fe_2O_{3(s)} + 3H_20$	III	Dehydration of amorphous ferric hydroxide to form hematite	
$Fe(OH)_{3(s)} \rightarrow \alpha\text{-}FeOOH_{(s)} + H_20$	III	Dehydration of amorphous ferric hydroxide to form goethite	
$2Fe^{2+}\ 0.5O_2 + 4OH^- \rightarrow 2FeOOH_{(s)} + H_2O$	III	Oxidation of ferrous iron to form goethite	Scale interior, scale surface layer
$3FeCO_{3(s)} + 0.5O_2 \rightarrow Fe_3O_{4(s)} + 3CO_2$	II and III	Partial oxidation of siderite to form magnetite (FeO·Fe2O3)	Scale interior, scale surface layer
$2FeCO_{3(s)} + 0.5O_2 + H_2O \rightarrow 2FeOOH_{(s)} + 2CO_2$	III	Oxidation of siderite to form goethite	Scale interior, scale surface layer

(AwwaRF and Wasser 1996; McNeill and Edwards 2001; Clement 2002; Sarin, Snoeyink et al. 2004)

Table 3 Iron solids found in corrosion scale layers

Iron Solids found in Scale	Oxidation State	Name
FeO	II	Wustite
α-FeOOH	III	Goethite
β-FeOOH	III	Akaganeite
γ-FeOOH	III	Lepidocrosite
$\alpha\text{-}Fe_2O_3$	III	Hematite
$\gamma\text{-}Fe_2O_3$	III	Maghemite
$FeO_x(OH)_{3-2x}$	III	Ferric oxyhydroxide
$Fe(III)_{x1}Fe(II)_{x2}(OH)_y(Cl^-, CO_3^{2-}, SO_4^{2-})_z$	II and III	"Green rust"
$FePO_4$	III	Strengite
$5Fe_2O_3 \cdot 9H_2O$	III	Ferrihydrite
Fe_4P	Unknown	Schrebersite

(McNeill and Edwards 2001; Sarin, Snoeyink et al. 2004)

1.2.1 FORMATION PROCESSES

Corrosion rates in new iron pipes are initially very high and eventually tail off as corrosion scale forms on the internal surface of the pipe, slowing the flow of oxidants to the pipe wall. Under conditions that promote uniform corrosion, a uniform scale layer can be seen to form. Localized corrosion results in the formation of 'mounds' of corrosion products typically referred to as tubercles (Sarin, Snoeyink et al. 2004). Tubercles may eventually grow into one another and form a seemingly uniform surface. While the corrosion reactions that occur with new iron pipes that result in the initial formation of corrosion scale are relatively straightforward and well understood, the reactions associated with aged (sometimes 50 or 100 years old) pipe can be more complex and dependent upon specific conditions. As noted in the AwwaRF report, "the longer a pipe has been in service, the more heterogeneous and complex the scale layer becomes and the more difficult it is to characterize the reactions of the corrosion products" (AwwaRF and Wasser 1996). Thus it can be seen that corrosion scale layers are dynamic and continually undergoing transformation.

Scale formation processes start with the corrosion of the pipe metal. The oxidized metal released as a result of the corrosion reactions serves as the material source for scale formations. During this stage of scale formation, oxidants have direct access to the metal pipe surface. Figure 3 below shows Pourbaix diagrams revealing the equilibrium conditions for selected ferrous and ferric species (where the total iron concentration equals 10^{-6} M). The diagram listed as (a) assumes that crystalline solids form where (b) includes the formation of amorphous solids. As metals precipitate, it is common for an amorphous, pseudo-stable solid to form first and then to convert to more stable, crystalline

forms over time. Note the potential (E_H) of waters containing 2 mg/L DO and 0.2 mg/L free chlorine. Assuming that these are minimum values for drinking waters, it can be inferred from these diagrams that there will always be a driving force to convert metallic iron to ferric iron when such water is in contact with the surface of the iron pipe (AwwaRF and Wasser 1996). During initial stages of corrosion, DO, free chlorine, and H^+ are the likely oxidants that contribute to corrosion (AwwaRF and Wasser 1996; Sarin, Snoeyink et al. 2004), while DO is likely the dominant oxidant (AwwaRF and Wasser 1996). Thus, the rate of corrosion is often thought of to be limited by the rate of diffusion of DO to the pipe surface. Figure 4 below provides a depiction of the initial stages of iron scale formation. In the diagram, DO and H^+ act to oxidize the metallic iron resulting in the release of ferrous (II) iron and the transfer of an electron, marked (A) and (C) in the diagram. In the presence of oxidants such as DO, ferrous (II) ions are further oxidized and hydrolyzed to form various ferric (III) (hydr)oxide phases (see (B) in Figure 4) (Sarin, Snoeyink et al. 2004).

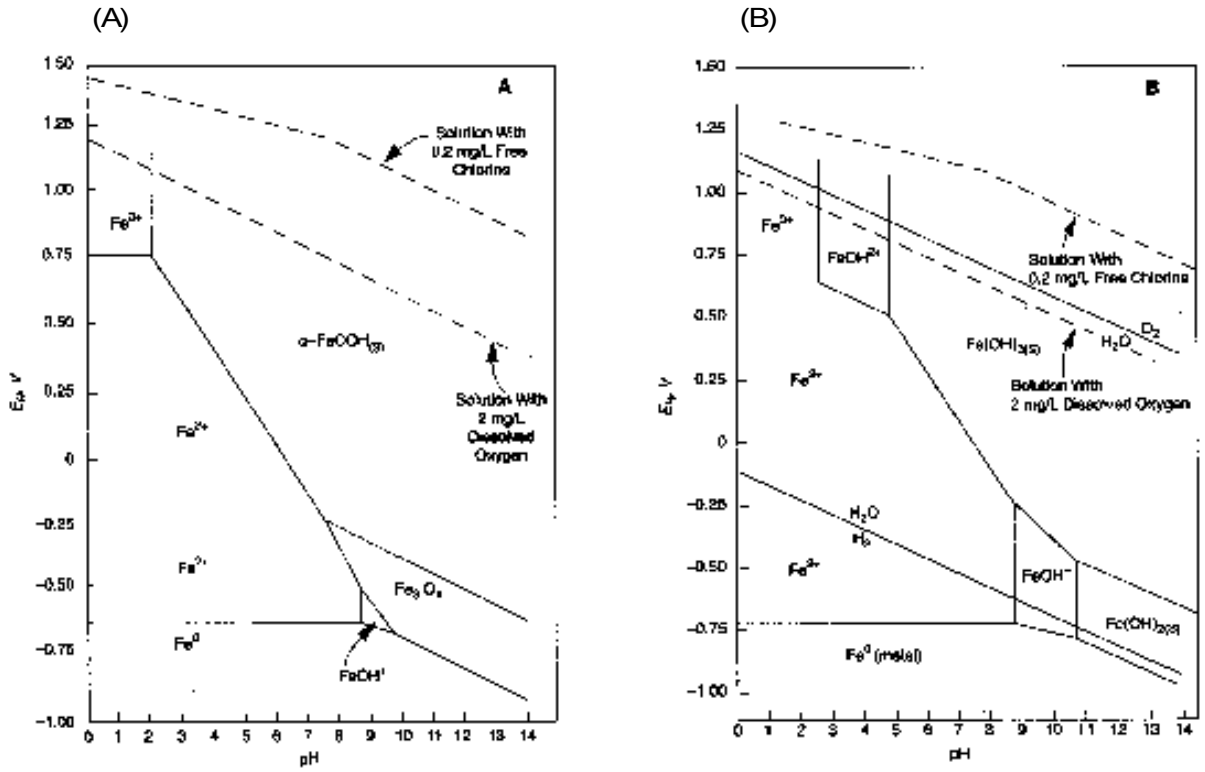

Note: Total soluble iron is 10^{-6} M (0.056 mg/L), and alkalinity is negligible. Diagram A is based on the assumption that crystalline solids might form; Diagram B assumes that only amorphous solids form. The dashed lines near the top of the diagrams indicate the E_H of solutions contained the indicated amounts of DO and chlorine.

Reprinted from *Internal Corrosion of Water Distribution Systems*, by permission. Copyright © 1996, American Water Works Association and Awwa Research Foundation.

Figure 3 Pourbaix diagrams for iron redox species

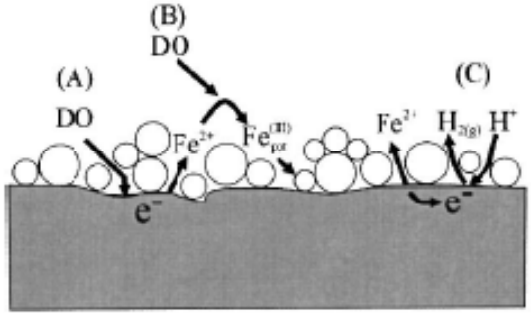

(Sarin, Snoeyink et al. 2004 With permission from ASCE)

Figure 4 Initial stages of iron scale formation

As detailed above, the conversion of solid iron to ferric iron does not occur directly. The fast oxidation of ferrous to form ferric (III) iron (see Figure 7 below) in presence of oxygenated water may either lead to the release of ferric iron into the bulk water or the accumulation of ferric iron on the pipe surface to form corrosion scale. The oxidation

reactions result in various iron oxide and hydroxide species including leidocrocite (γ-FeOOH), goethite (α-FeOOH), ferric hydroxide ($Fe(OH)_3$), ferrihydrite ($5Fe_2O_3 \cdot 9H_2O$), magnetite (Fe_3O_4), maghemite (γ-Fe_2O_3), and others (Clement 2002; Sarin, Snoeyink et al. 2004). Green rust, which includes both ferrous and ferric iron phases, may also form (Sarin, Snoeyink et al. 2004). A variety of factors may determine the specific mineral phase formation, and may include the rate of oxidation, pH, concentration of ferrous ions, and the concentration of other species in solution (Cornell and Schwertmann 1996; Sarin, Snoeyink et al. 2004). Table 4 below identifies favorable conditions for the formation of various mineral phases formed from ferrous (II) iron oxidation.

Table 4 Conditions for favorable formation of mineral products from oxidation of ferrous Iron

Mineral	Chemical Formula	CO_2 Present	CO_2 Absent	Slow Oxidation	Fast Oxidation	Lower pH	Higher pH	pH>5	pH<5	Low [Fe^{2+}]	High [Fe^{2+}]
Goethite	α-$FeOOH_{(s)}$	X		X		X					
Lepidocrocite	γ-$FeOOH_{(s)}$			X				X			
Lepidocrocite	γ-$FeOOH_{(s)}$				X	X				X	
Lepidocrocite	γ-$FeOOH_{(s)}$		X		X		X				
Ferrihydrite	$5Fe_2O_3 \cdot 9H_2O$				X				X		
Magnetite	Fe_3O_4			X			X				X

(Cornell and Schwertmann 1996)

As mentioned previously, localized corrosion results in the formation of tubercles on the internal surface of the pipe. During initial stages of corrosion, tubercles are not uniform across the pipe surface. In locations where tubercles form, oxidants are limited from flowing freely to the pipe surface. In regions where no scale layers form, oxidants are

still able to easily diffuse to the pipe surface. The result is an oxidant concentration cell in which the iron metal dissolves at the anodic site and electrons are released at cathodic sites that are oxidant rich (Sarin, Snoeyink et al. 2004). Localized corrosion of the iron metal is maintained under these conditions. As corrosion continues and tubercles grown, a shell-like layer is formed on the surface of the tubercle. The dense, shell-like material is made of up oxidized species such as magnetite and goethite (Sarin, Snoeyink et al. 2004) which serve to further prevent the flow of oxidants to the pipe surface. Ions may continue to pass through the shell-like layer in order to maintain electroneutrality. Figure 5 below shows a depiction on the intermediate state of corrosion scale formation. Note that the gray shaded rectangular shapes correspond to the particles that make up the shell-like layer. Ions are represented as A^{n-} and anodic and cathodic sites are shown at the site of electron release and acceptance respectively.

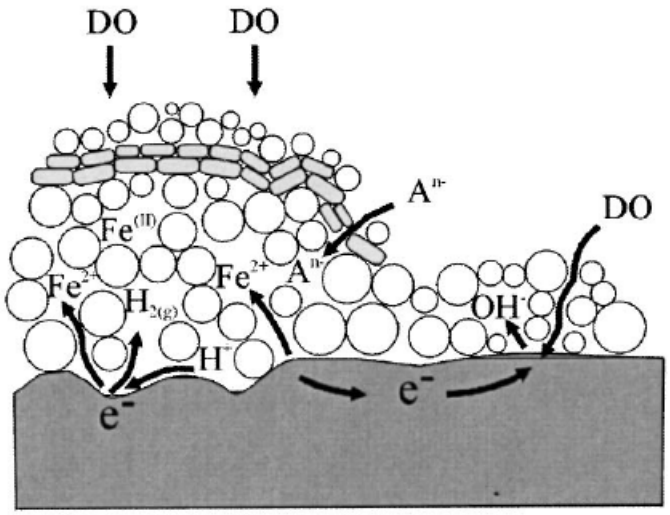

(Sarin, Snoeyink et al. 2004 With permission from ASCE)

Figure 5 Intermediate stages of iron scale formation

As corrosion continues, ferrous (II) ions from at the anode of the pipe surface are released into the interior of the scale. The fate of these ions depends on a number of

factors. A number of possible pathways are presented above in Table 2. Ultimately, ferrous ions released from the corrosion reaction end up either as ferrous, ferric, or a mixed ferrous-ferric phase. As the tubercle develops the dense outer shell-like layer, oxidants are prevented from flowing through the scale. The result is a gradient of mineral iron oxidation states ranging from Fe(III) at the scale surface to Fe(II) at the pipe surface (Sarin, Snoeyink et al. 2004). The rate at which the released ferrous (II) ions are oxidized can depend on the pH, the availability of oxidants, or other factors. Ions that are released into the bulk water experience high oxidation rates and form ferric hydroxide as well as possibly lepidocrocite (Sarin, Snoeyink et al. 2004). Slower oxidation rates are generally found in the interior of the scale and result in the formation of goethite, hematite, lepidocrocite, magnetite, and green-rust (which includes both ferrous and ferric iron) phases (Sarin, Snoeyink et al. 2004). These mineral phases eventually form the dense shell-like layer. Once the shell-like layer is developed, the prevention of oxidants into scale results in reducing conditions in the interior scale core. Ferrous mineral phases such as siderite ($FeCO_{3(s)}$) and ferrous hydroxide ($Fe(OH)_{2(s)}$) dominate in these locations (Sarin, Snoeyink et al. 2004). Intermediate sections of scale may contain mixed mineral phases of ferrous and ferric compounds such as green rust or magnetite.

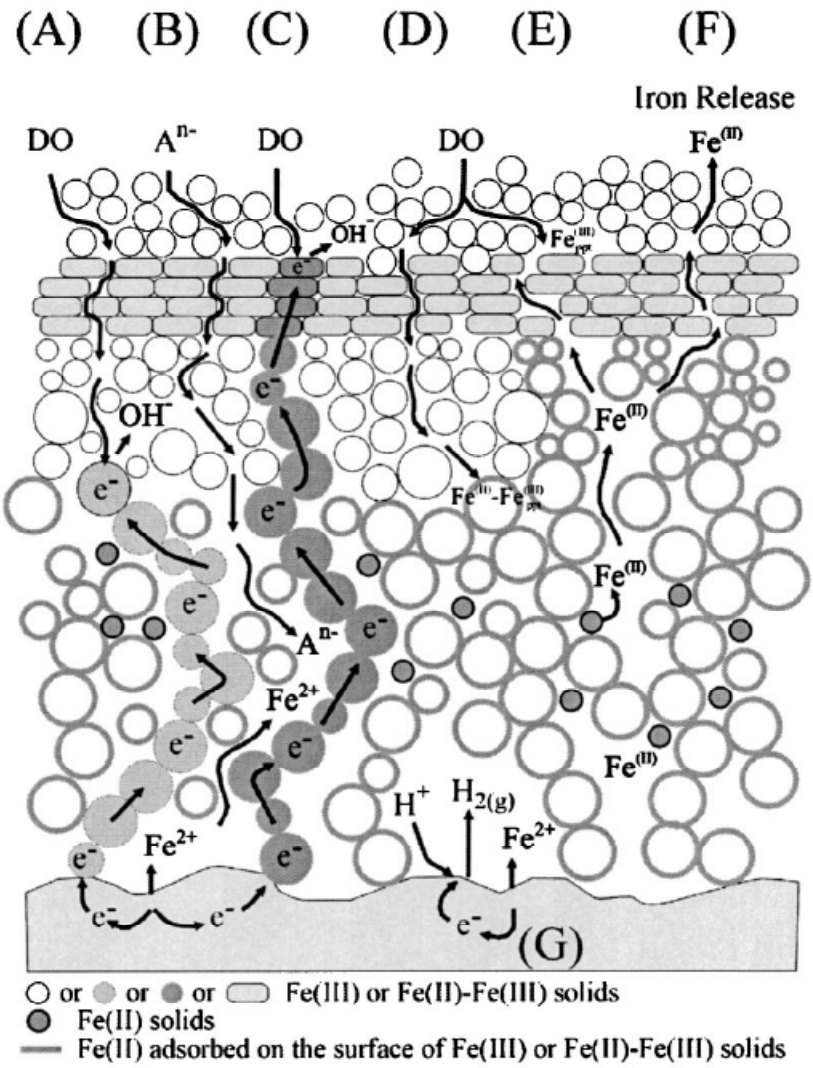

(Sarin, Snoeyink et al. 2004 With permission from ASCE)

Figure 6 Schematic depiction of mature iron corrosion scale and possible pathways for iron release under normal flow conditions

1.3 Factors Influencing Red Water Events

As mentioned previously, red water problems are generally the result of a combination of water chemistry, biological processes, composition of pipe scale, and the hydraulic flow characteristics within the pipe. This section intends to present the available knowledge regarding each of these in relation to iron scale release processes that lead to red water problems.

There is still some disagreement among experts as to the specific mechanisms that are responsible for scale release in iron pipes. The following excerpts were taken from scholarly literature published in 2002, 2003, 2003, 2004, 2003, and 1996 respectively.

> *"Iron release occurs when ferrous phases in the scale dissolve, and water quality conditions permit the ferrous ion to diffuse into the bulk water in contact with the pipe." and later "…the mechanisms for iron release into bulk water to form red water are not fully understood. Iron release can be affected by water quality parameters… It can also be influenced by the physico-chemical nature of the corrosion scale ."* (Clement 2002)[2]

> *"The sensitivity of iron release to alkalinity changes … supports the idea that dissolution of carbonate-containing iron phase in the corrosion scales is a possible mechanism for iron release from corroded pipes."* (Sarin, Clement et al. 2003)

> *"The effects of water quality parameters, notably chlorides, sulfates, and dissolved carbon … along with the hydraulic conditions within the pipe system, lead to the release of iron from the passive corrosion product layer in particle form."* (Mutoti 2003)

[2] See page 31 of citation. The authors also note the role of hydraulic forces in scouring scale and resuspending particles.

"Iron release refers to the transport of iron, either in soluble or particulate form, from the corroded pipe metal to the bulk water." (Sarin, Snoeyink et al. 2004)

"Discolored water can occur only if a source of particulate matter is present and if the hydraulic conditions promote sedimentation and occasional resuspension… Discolored water incidents are the result of sediment resuspension in the network." (Slaats, AwwaRF et al. 2003)

"…ferric hydroxide flocs rather than crystalline scale are found in red waters. High concentrations of ferrous ions are also often observed in such waters, especially where no free chlorine residual is available. This suggests that many red-water problems arise through oxidation of ferrous ions in the bulk solution and the subsequent precipitation of ferric hydroxide, rather than by release of preformed particles from the existing scales. The ferrous ions could form at the metal surface or within the scales and then be transported into the bulk water phase by diffusion." (AwwaRF and Wasser 1996)

These excerpts provide some insight into the disagreement concerning iron release processes as well as the difference into research priorities. Does iron release occur primarily from water chemistry process (such as dissolution/precipitation processes and redox interactions)? Or are hydraulic processes (scouring, suspension, settling, resuspension) the primary culprit? Is it a combination of all of these factors? Should research be focused on the processes/mechanisms involved in maintaining water

chemistry that lessens red water problems or should efforts be focused on understanding how to mitigate resuspsension of particulate in the network? The following sections intend to provide the current understanding regarding the various factors influencing iron scale release.

1.3.1 HYDRAULICS

The flow regime within a pipe typically affects iron scale release under either stagnant/dead end conditions or under conditions of high (turbulent) flow. Low flow / dead end / stagnant conditions result in the depletion of dissolved oxygen and chlorine within the bulk water and at the pipe surface. The lack of oxidants results in reducing conditions in the scale. Ferrous species are thus favored which results in a more porous surface layer of scale (see Sec. 1.2). This provides for an increase in ferrous iron release (Burlinkgame, Lytle et al. 2006). Dissolved ferrous species can be oxidized afterward if mixed with oxidant rich waters resulting in ferric particulate (red water). Under typical flow conditions, where dissolved oxygen and chlorine residual are maintained, ferrous species that are released from the interior of the scale are typically oxidized and form the denser shell like layer at the surface of the scale.

While turbulent / high flow conditions may increase the corrosion rate of the iron pipe by continually supplying oxidants to the pipe surface, after mature scale is developed, the constant supply of oxidants aids in development of denser protective scale (McNeill and Edwards 2001). At high enough flow velocities though, the shear stress applied to the pipe wall can result in the scouring away of protective scaling. Note the following guidelines for unidirectional flushing in distribution systems (Kirmeyer 2000):

- ≥ 3 ft/sec – remove silts, sediment, reduce disinfectant demand

- ≥ 5 ft/sec – promote scouring, remove biofilm, loose deposits, reduce disinfectant demand
- ≈ 12 ft/sec – remove sand from inverted siphons

Other studies have attempted to identify the water velocity capable of maintaining particles in suspension. This approach assumes that a significant source of red water causing material exists as loose deposits within the distribution system. At low velocities, particles may experience gravitational settling and accumulate on the surface of pipes in low flow regions. Higher velocities allow for particles to be maintained in suspension and even result in settled particles to be re-suspended. Boxall and Dewis have outlined much of the research coordinated to identify velocity criteria for particulate transport in pipes (Boxall and Dewis 2005). They note the work done by Ackers *et al* to report the velocity at which particle motion was initiated in various diameter pipes (Ackers, Brandt et al. 2001). Many other studies have investigated the terminal velocity of particles through stagnant water, the rate of settling of particles under laminar flow conditions (which incorporate the Saffman and Magnus lift forces), the fate of particles under turbulent flow conditions, the velocity required for re-suspension of settled particles, the effect of pipe diameter, and the correlation of water velocity to required shear stress resulting in entrainment of particles from a sediment bed (Shields 1936; Vanoni 1975; Shook and Roco 1991; Fan and Zhu 1998; Subhasish 1999; Jayaratne, Ryan et al. 2004).

It should be noted that disagreement currently exists regarding the settling ability of particles in the distribution system. Jayaratne, Ryan, et al. (2004) discuss the effect of gravitational settling of particles in a water distribution system under low or no flow conditions. Conversely, Boxall and Saul (2005) cite that the terminal velocities for the

range of typical particle sizes in a WDS are orders of magnitude lower than the forces generated by laminar and turbulent flows typical in distribution systems. They note that totally quiescent conditions would be required for greater than two hours for an average sized particle to settle in a 100 mm diameter pipe.

1.3.2 WATER CHEMISTRY RELATED

The following list is not intended to be a comprehensive list of water chemistry parameters that affect iron scale release. As mentioned previously, the specific processes and mechanisms responsible are not all fully understood. The list below provides insight into parameters that are thought to have significant effects on iron scale release.

pH

The role of pH in iron scale release is still under investigation, although specific processes have been proposed. Sarin and others were able to show that as pH increases, iron release in unlined cast iron pipes decreases. They suggest that this could be due to the fact that the solubility of ferrous (ferrous hydroxide and ferrous carbonate) solids within the scale decreases as pH increases. If dissolution of these solids is a primary mechanism for iron scale release, then increasing the pH should reduce the amount of iron released. A decrease in iron release has been observed when pH was increased from 7.5 to 9.5 in a pipe loop study of aged iron pipe (Sarin, Snoeyink et al. 2004). It has also been suggested that lower pH results in the formation of more porous scale structure while a higher pH resulted in a denser, sturdier scale. This suggests that an increase in pH would decrease iron release (Baylis 1926; Sarin, Clement et al. 2003).

The pH dependence of iron oxidation kinetics has also been suggested to influence iron scale release. Ferrous iron oxidation rates increase with increasing pH (see Figure 7).

As dissolved ferrous iron within the scale migrates toward the scale surface, high pH will allow rapid oxidation to ferric particulate that reinforces the dense shell-like surface scale. At lower pH, slower oxidation rates could allow dissolved ferrous species to diffuse past the surface layer into the flowing water (AwwaRF and Wasser 1996; Sarin, Clement et al. 2003). Other thermodynamic, kinetic, or dissolution/precipitation water quality variables may show a strong dependence upon pH.

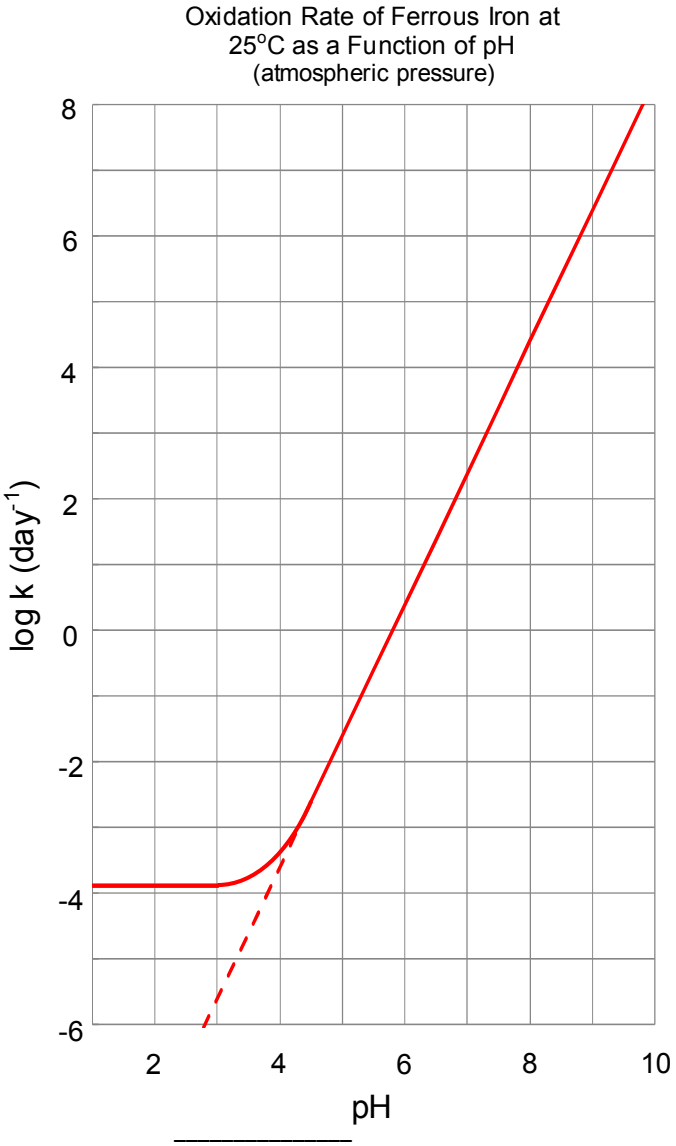

Figure 7 Ferrous iron oxidation kinetics as a function of pH

Alkalinity

Alkalinity is generally thought of to have mitigating effects on corrosion release. Experiments conducted at a pilot water distribution system in Tampa, FL revealed that alkalinity has an inverse relationship with iron release in aged iron pipes (Imran, Dietz et al. 2005). Another study found that under certain conditions, iron release increased by 50 – 250% immediately when alkalinity was decreased from 30-35 mg/L as $CaCO_3$ to 10-15 mg/L as $CaCO_3$ (under constant pH) (Sarin, Clement et al. 2003). The specific processes controlling the role of alkalinity in iron scale release are not entirely understood at the moment. Sarin and others suggest that the link between alkalinity and iron scale release has to do with the dissolution of carbonate containing iron phases within the scale (such as siderite). This concept is based on the assumption that iron release is dominated by dissolution of ferrous species within the scale. Under this thinking, siderite, being the most soluble ferrous species, dominates the dissolution of ferrous species. Higher alkalinity (carbonate) concentrations would then mean that less siderite ($FeCO_3 \rightarrow Fe^{2+} + CO_3^{2-}$) could be dissociated under equilibrium conditions. (Sarin, Clement et al. 2003)

Chloride Ion Concentration

Burlingame, Lytle, and Snoeyink note that while oxidants are typically prevented from passing through the dense outer scale layer, chloride anions are capable of passing this barrier in order to maintain electroneutrality (Burlinkgame, Lytle et al. 2006). The presence of chloride in the inner core produces acidic conditions that provide for further corrosion of the pipe surface (release of ferrous species). They note that short term increases in chloride content have resulted in increases in iron release.

Additionally, chloride content is a variable in the Larson index. Studies by Larson found that increases in chloride (and sulfate) relative to bicarbonate made water more corrosive. Corrosivity does not necessarily correlate to scale release problems though. McNeill and Edwards conclude that the role of chloride in corrosion and red water issues is not completely understood. They cite studies that have shown that chloride increases diffusion of ferrous iron through scale as well as others that conclude that chloride causes a more protective scale to form on steel surfaces (McNeill and Edwards 2001).

DO Content

Studies have shown that increasing the levels of dissolved oxygen (as well as other oxidants) reduce the amount of iron release from corroded iron pipes (Sarin, Snoeyink et al. 2004). As oxygen rich water interacts with the scale surface, ferrous species are oxidized resulting in the formation of a dense shell layer. This dense outer layer can prevent the diffusion of oxygen to the porous core of the scale as well as the pipe surface (limiting further corrosion). This results in reducing conditions in the porous core. Reducing conditions favor formation of more porous ferrous iron species. The dense outer layer may also prevent the diffusion of dissolved ferrous species from the porous core from being released into the bulk water. In water depleted of oxygen (and other oxidants), reducing conditions at the outer layer of the scale favor formation of soluble ferrous species. This provides for greater opportunity for iron release via dissolution of the outer scale layer. Also, the lack of a dense outer scale layer provides no barrier for the transport of dissolved ferrous species from the porous core of the scale to the bulk water. (Burlinkgame, Lytle et al. 2006)

Temperature

Temperature can have a variety of effects on iron scale release. Temperature can affect release by altering the thermodynamics of reactions occurring in the scale. The hierarchy of reactions may be significantly influenced by temperature. Additionally, the physical properties of the scale could be affected by temperature. Scale that is subjected to fluctuations in temperature could experience repetitive thermal expansion and contraction that could lead to cracking. The influence of temperature on kinetics could influence iron scale release. The inevitable increase in reaction rate as temperature increases could correlate to increases in reaction processes (ex. rate of scale dissolution increases with increasing temperature). Indirectly, temperature affects the solubility of dissolved oxygen, the thermodynamics of corrosion reactions, viscosity of water, oxidation rates, and biological activity. Studies have generally shown that iron release increases with increasing temperature (McNeill and Edwards 2001; McNeill and Edwards 2002).

Sulfate Concentration

Sulfate is a variable included in the Larson index. This index was created to indicate the corrosivity of a particular water and refers to the ration of sulfate and chloride to bicarbonate:

$$Larson\ Index = \frac{2[SO_4] + [Cl]}{[HCO_3]}$$

A higher value for the Larson index indicates a more corrosive water. As mentioned previously though, while sulfate may increase corrosion rates, its effect of corrosion scale release is not directly correlated. Burlingame and others discuss the role of sulfate reducing bacteria (which reduce sulfate to sulfide) in altering the composition of the

corrosion scale. This is discussed further in Section 1.3.4 below. McNeill and Edwards conclude that the role of sulfate in corrosion processes is not completely understood yet. While certain studies have shown that the presence of sulfate increases ferrous iron diffusion into delivered water, others have shown that sulfate inhibits the dissolution of iron oxides and aids in the development of denser, more protective scale.(McNeill and Edwards 2001)

Calcium Concentration

Historically, calcium has been thought to aide in corrosion release mitigation. The Langelier Index (LI) has been utilized to stabilize waters according to calcium carbonate precipitation. The thought is that waters that are slightly oversaturated with calcium carbonate ($CaCO_3$) will precipitate a thin, protective calcite layer on the surface of iron scale preventing further corrosion. Calcium could be added to increase the LI, thus "stabilizing" the water.

Despite continued use, the LI has been discredited as a useful tool for preventing iron scale release problems (AwwaRF and Wasser 1996; McNeill and Edwards 2001). While the use of the LI may provide information for saturation of calcium carbonate, corrosion and corrosion release processes tend to be very complex and site specific.

1.3.3 THE KUCH MECHANISM

Following the development of the siderite model, Kuch observed that corrosion processes and scale dissolution in aged iron pipes still continue in situations where oxygen is completely depleted (due to stagnation) at the metal surface. He suggested that an alternative mechanism is responsible for corrosion and iron release in oxygen/oxidant depleted waters. He hypothesized that ferric oxides were a logical candidate to be an

electron acceptor. Kuch suggested that during periods of stagnation, the anodic corrosion reaction (oxidation of iron metal) was maintained by the cathodic reduction of ferric oxides in the scale.(AwwaRF and Wasser 1996)

-Anodic reaction: $Fe_{(s)} \leftrightarrow Fe^{2+} + 2e^-$

-Cathodic reaction: $2FeOOH_{(s)} + 2H^+ + 2e^- \leftrightarrow 2Fe^{2+} + 4OH^-$

-Overall reaction: $Fe_{(s)} + 2FeOOH_{(s)} + 2H+ \leftrightarrow 3Fe^{2+} + 4OH^-$

Note that both the anodic and cathodic reactions result in the formation of dissolved ferrous iron. Under reducing conditions of stagnant water, dissolved ferrous iron is maintained at a reduced state and may be transported into the bulk water. As flow resumes, oxidant rich waters act to oxidize the ferrous ions, resulting in characteristic red water.

Sarin and others have expanded on this research more recently by investigating the role of scale microstructure and composition on the release of iron in water distribution systems (Sarin, Snoeyink et al. 2001; Sarin, Snoeyink et al. 2004; Sarin, Snoeyink et al. 2004).

1.3.4 BIOLOGICAL FACTORS

Biological activity on pipe surfaces in a water distribution system may have a variety of results but are generally thought to have detrimental effects regarding iron corrosion and scale release (McNeill and Edwards 2001). In general, microbes in scale layers can be iron reducing or iron oxidizing, affecting scale composition. Additionally, microbes can consume oxygen (or other oxidants such as chlorine) and alter pH, also resulting in alterations in scale composition (McNeill and Edwards 2001). Anaerobic or near anaerobic conditions within the scale provide a favorable environment for the growth

of sulfate reducing bacteria (SRB). SRB reduce sulfate to sulfide. When sulfide interacts with ferrous iron, pyrite (FeS_2) is formed. This reduces the magnetite content of the scale and can result in a more loose porous scale structure (Burlinkgame, Lytle et al. 2006).

1.3.5 Corrosion Inhibitors

Phosphate corrosion inhibitors were introduced decades ago to limit excess calcite precipitation in water distribution systems. It was later discovered that phosphate inhibitors also limit iron precipitation and corrosion (McNeill and Edwards 2001). Phosphate inhibitors used over the years include hexametaphosphate (polyphosphate), orthophosphate, zinc orthophosphate, zinc metaphosphate, and bimetallic phosphate (sodium-zinc or potassium-zinc) (McNeill and Edwards 2000). The limiting mechanism accomplished by phosphate inhibitors is not thoroughly understood at this point, although many theories have been suggested (McNeill and Edwards 2001). Sarin et al note that it has been suggested that orthophosphate inhibitors form insoluble phosphates in scale layers that increase impermeability and that inhibitors have been effective in iron, galvanized iron, lead, and copper pipes (Sarin, Clement et al. 2003). It has been observed that under stagnant flow conditions, the addition of phosphate inhibitors has no effect or a detrimental effect on iron release (McNeill and Edwards 2000).

1.3.6 Summary of Iron Release Mechanisms/ Processes

Figure 8 below identifies pathways resulting in red water formation. In general, iron particles resulting in characteristic red water may be the result of iron entering the distribution system from the source water (either from treatment operations or some other source) or as a result of the release of iron corrosion scale layers from pipe surfaces within the distribution system. The fate of iron in the WDS is affected by a variety of

hydraulic, chemical, and biological factors. Iron particles in suspension may accumulate on a pipe surface or be maintained in suspension (depending on flow conditions). Additionally, iron may be released from corrosion scale layers in the reduced (ferrous) form. As ferrous irons mix with oxidants in the bulk water, highly insoluble ferric species form. As such, red water events may result from particulate suspension or resuspension events or may also be the result of corrosion scale release processes.

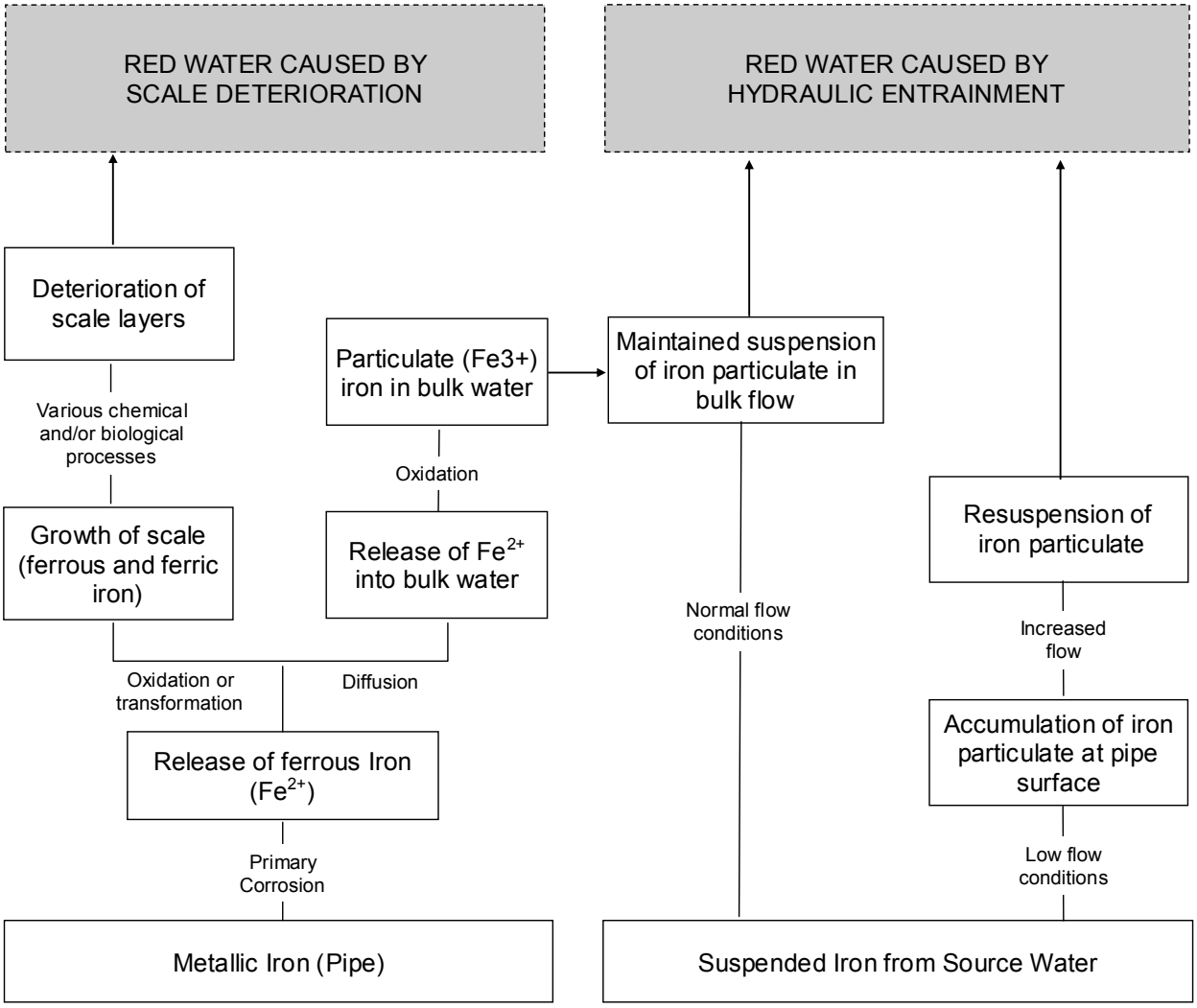

(AwwaRF and Wasser 1996; Wricke, Henning et al. 2007)

Figure 8 Red Water Pathways

2. Effects of Internal Iron Pipe Corrosion

2.1 Aesthetic Effects (Taste & Odor)

Aesthetic concerns regarding water quality deal with taste and odors as well as the appearance delivered water. Iron corrosion in water distribution systems is known to cause metallic taste and musty odors (Kirmeyer 2000). Red colored water is probably the most common result of corrosion. Red water events occur when iron corrosion particles are released into the bulk water. In addition to an unpleasant appearance, red water can stain laundry and plumbing fixtures. Black water may also be a result of iron corrosion. Black water forms from ferrous species of iron. Iron persists as ferrous species when oxygen is depleted and not present to oxidize to ferric iron (red color) (Kirmeyer 2000).

The role of corrosion scale in chlorine consumption may also have implications on consumer perception of water taste. Degradation of chlorine disinfectant occurs as a result of chemical reactions with constituents in the water as well as reactions with materials at the pipe surface. Chlorine degradation specifically related to reaction with the pipe material, biofilms, and tubercules is known as wall demand (Al-Jasser 2006). Wall demand is likely the primary reason for chlorine disinfectant degradation in the distribution system (DiGiano and Zhang 2005a). While excess of chlorine is a leading cause of customer complaints and dissatisfaction with drinking water (Piriou, Mackey et al. 2002), any alterations to drinking water quality may affect the consumer perception of water taste and/or odor. A recent study found that the measured sensitivity of average Americans to free chlorine and chloramines in tap water were 0.8 and 3.7 mg/L Cl2 respectively (Mackey, Baribeau et al. 2002). No studies investigating the sensitivity of Americans to

changes in chlorine disinfectant concentration are available at this point. Alterations in the distribution system due to increased corrosion, corrosion scale release, or changes in scale composition make influence wall demand. It is likely that these alterations in wall demand may affect consumers' preference with regard to water taste. If this is the case, it is possible that consumer complaint data could be used to identify potential corrosion problems in the distribution system.

The presence of sulfides also cause taste and odor problems in delivered water. Sulfides result in a rotten egg odor. Additionally sulfides may accelerate corrosion processes by reacting with metallic ions resulting in nonprotective insoluble sulfides that can deteriorate metal pipe surfaces. This process can result in black colored water. (Kirmeyer 2000)

2.2 Health Effects

Iron in drinking water poses no direct threat to human health. This is reflected in the fact that no primary drinking water standard has been established for iron in drinking water. A secondary standard of 0.3 mg/L is recommended by the EPA for cosmetic purposes (USEPA 2008). While iron release in drinking water has no direct effect on human health, there are some significant health concerns that are related to corrosion processes. Internal iron corrosion and the release of iron corrosion scale into the bulk water inevitably consume dissolved oxygen and disinfectant. Added demands for oxygen and disinfectant could provide for conditions necessary for harmful biofilm growth. Additionally, iron pipe inevitably contains small amounts of potentially harmful materials such as arsenic and radium. As the pipe corrodes, the composition of the resultant scale

will includes these substances. Scale release processes then provide a means for these harmful substances to end up in the water supply. (Sarin, Snoeyink et al. 2004)

2.3 Changes to Iron Pipe

Corrosion of iron pipes results in a variety of (typically harmful) alterations to the pipe. As corrosion scales form, the hydraulic capacity of the pipe is lowered resulting in higher pumping costs. This could eventually require replacement of the pipe at high cost to the utility. Corrosion can also lead to pipe failure when localized corrosion processes cause ruptures in the pipe (this is especially true with galvanized pipes). This also requires costly pipe replacement as well losses in delivered water that is released.

3. Iron Corrosion Release Models

Modeling of red water events is important for recognizing possible water quality problems as well as identifying deterioration in the WDS. Additionally, red water and discolored water remain one of the largest causes of customer complaints for water utilities. The ability to accurately predict scale release and particulate transport could be greatly utilized by utilities to avoid or minimize these occurrences. Currently, there are no widely available packages for modeling corrosion release or particulate transport within a water distribution system. All modeling efforts identified to date are relatively recent developments. Models discovered to date may emphasize the rate of iron release from scale, the suspension and resuspension of settled particles in pipes, or some other variable. A summary of each model is included below. Note that the Statistical Red Water Release Model (3.1) and the Iron Release Flux Model (3.2) were developed concurrently to allow

for an iron release determination based on water quality parameters as well as pipe material and hydraulics.

3.1 Statistical Red Water Release Model

The statistical red water release model was developed at the University of Central Florida to predict the effect of influent water chemistry on iron scale release in the WDS. This research was conducted to help evaluate whether changes in source water blends will result in unacceptable changes to water quality within the distribution system. Due to recent implementation of groundwater conservation measures, water utilities that have depended on groundwater in the past will be face with considering alternative sources to supplement the primary supply. (Imran, Dietz et al. 2005).

A pilot distribution system was constructed using excavated aged pipes from various water utilities surrounding Tampa, FL. Eighteen different lines were constructed (average length 91ft) made up of unlined cast iron, lined cast iron, galvanized pipe, and PVC pipe. Experiments measured changes in apparent color (CPU) across pipe reaches for varying source water blends. Apparent color was used as a surrogate for total iron concentrations. The researchers observed that total iron concentrations were dominated by particulate forms of iron and that total iron showed a strong correlation to the change in apparent color. Varying blends of seven different source waters were used for experiments. All source waters were chloraminated and stabilized to maintain a positive LI. The project was divided into five three month phases. Phases 1 – 3 operated at a five day HRT to simulate dead ends/ stagnant water. Phases 4 – 5 operated at a two day HRT to allow for chlorine residual maintenance. (Imran, Dietz et al. 2005)

To develop this model, an ANOVA was used to identify significant parameters. Parameters included in the model include dissolved oxygen, conductivity, sulfate ion concentration, chloride ion concentration, sodium ion concentration, temperature, HRT, alkalinity, calcium ion concentration, silica content (SiO_2), UV_{254} (cm^{-1}), and pH. The final model was selected based on the results of the ANOVA and can be seen below. Significant parameters include chloride concentration, sodium concentration, sulfate concentration, dissolved oxygen, temperature, HRT, and alkalinity. (Imran, Dietz et al. 2005)

$$\Delta Color = \frac{[Cl^-]^{0.485} * [{SO_4}^{2-}]^{0.118} * [Na^+]^{0.561} * [DO]^{0.967} * T^{0.813} * HRT^{0.836}}{20.9411 * [Alk]^{0.912}}$$

Note that calcium and pH were not identified as significant variables, contrary to conventional expectations. The authors cite that this is due to the fact that all waters were stabilized to a positive LI and all waters had a narrow pH range (Imran, Dietz et al. 2005).

3.2 Iron Release Flux Model

The iron release flux model was also developed by researchers at the University of Central Florida. This group has developed a model for iron release in WDS that simulates iron concentration based on a novel surface release flux term, pipe material, pipe geometry, and hydraulic retention time. This model proposes that iron scale is released into delivered water via film release processes. Thus, a zero order kinetic model has been proposed that quantifies the mass flux of iron release (as particulate) from scale layers. (Mutoti 2003; Mutoti, Dietz et al. 2007a; Mutoti, Dietz et al. 2007b)

Experiments were conducted using the same Pilot Distribution System used for the statistical red water release model and intended to estimate the magnitude of the flux term. A single source water blend incorporating 60% conventionally treated water, 30%

enhanced treated surface water, and 10% desalinated RO water was used during experiments. Turbidity measurements served as a surrogate for total iron concentration. Mass flux calculations were obtained by correlating changes in turbidity across pipe segment to changes in total iron concentration. This assumes that total iron concentration is dominated by particulate forms of iron, which was shown in the experimental results. The relationship between total iron concentration and turbidity is as follows:

$$\Delta Fe(ug/L) = \frac{\Delta Turbidity\ (NTU)}{7.3x10^{-3}}$$

From this calculation and knowing the flow rate and pipe length and diameter, the flux term could be estimated. (Mutoti 2003; Mutoti, Dietz et al. 2007a)

The flux term (K_m) is defined as the iron mass rate of release per unit area and has units of mg/(m^2.day). Iron concentration in water exiting the distribution pipe is directly proportional to the flux term and the hydraulic retention time (HRT) in days and inversely proportional to the pipe diameter (m). The predicted iron release is determined by the equation below[3] (Mutoti 2003; Mutoti, Dietz et al. 2007a):

$$\Delta[Fe] = \frac{4K_m HRT}{D}$$

The resulting units for increase in iron concentration (Δ[Fe]) are mg/m^3. This increase in iron concentration correlates to an increase in total iron, although it is assumed that particulate forms of iron dominate. Flux term determination was carried out through a series of experiments incorporating two pilot distribution systems (galvanize pipe and cast iron) and a blend of treated water (30% surface, 60% groundwater, and 10% saline).

[3] The flux equation was derived from the Advection Dispersion equation as well as a steady state mass balance equation. See Appendix A for these derivations.

Turbidity measurements served as a surrogate for total iron concentration. This implies that particulate forms of iron dominate the total iron concentration. Mass flux calculations were obtained by correlating changes in turbidity across pipe segment to changes in total iron concentration. From this calculation and knowing the flow rate and pipe length and diameter, the flux term could be estimated. It is important to note that pipes were flushed to remove any existing sediment prior to recording turbidity measurements. Thus, these experiments intend to solely measure iron scale release and show no indication of the potential to resuspend iron particulate that has settled in the distribution system. (Mutoti 2003; Mutoti, Dietz et al. 2007a)

Good correlation was found between predicted and observed iron concentrations for waters exiting the pilot distribution systems. The experimental flux term showed a distinct change in relationship at a Reynolds number equal to 2000. This is the traditional threshold between laminar and turbulent flow. Thus, a piecewise model is necessary, one relationship for laminar flow, another for turbulent flow. For galvanized pipe and Reynolds number at or below 2000, the flux term remained constant at 1.99 mg Fe/m^2.day. Similarly for cast iron pipe under laminar flow conditions, the flux term remained constant at 4.16 mg Fe/m^2.day. For Reynolds numbers greater than 2000, the flux term was fit to a linear regression that was constrained to the average constant flux value under laminar flow conditions for both pipe material types considered. These values can be seen in Table 5 below. PVC and lined cast iron pipes were also evaluated for flux term determination, but iron release was found to be negligible. (Mutoti 2003; Mutoti, Dietz et al. 2007a)

Table 5 Flux term values for varying pipe material and flow patterns

	Galvanized Pipe	Cast Iron
Laminar Flow (Re<2000)	1.99	4.16
Turbulent Flow (Re>2000)	0.0045*(Re-2000)+1.99	0.009*(Re-2000)+4.16

(Mutoti 2003)

In order to incorporate changes to water chemistry, the statistical red water release model can be used in conjunction with the flux model (Mutoti 2003; Imran, Dietz et al. 2005; Mutoti, Dietz et al. 2007a). The flux term is altered by incorporating the UCF statistical model equation below to predict change color release in the absence of measured values.

$$\Delta C = \frac{[Cl^-]^{0.485} * [SO_4{}^{2-}]^{0.118} * [Na^+]^{0.561} * [DO]^{0.967} * T^{0.813} * HRT^{0.836}}{20.9411 * [Alk]^{0.912}}$$

Color release is assumed to be directly proportional to the flux term, whereas

$$\frac{K_{m_1}}{K_{m_2}} = \frac{\Delta C_1}{\Delta C_2}, \text{ and therefore } \quad K_{m_2} = K_{m_1}\frac{\Delta C_2}{\Delta C_1} \text{ (Mutoti 2003)}$$

The water chemistry parameters for the water used to determine the flux term values in Table 5 above are as follows: $[Cl^-]_{(1)}$ = 38 mg/L, $[SO_4{}^{2-}]_{(1)}$ = 66 mg/L, $[Na^+]_{(1)}$ = 31 mg/L, $[DO]_{(1)}$ = 7.5 mg/L, $T_{(1)}$ = 20°C, $HRT_{(1)}$ = 5 days, $[Alk]_{(1)}$ = 148 mg/L as $CaCO_3$, and $\Delta Color_{(1)}$ = 9.34 CPU (Mutoti 2003). Since K_{m1} and ΔC_1 are known values determined during the flux experiments and ΔC_2 can be calculated based on water quality parameters using the statistical model, the flux term (K_{m2}) may be adjusted for any source water.

The flux model was verified using fourteen independent hybrid pilot distribution systems each with varying pipe materials and varying source water chemistries over a four phase year long testing period. Results showed good results for waters with similar chemical makeup to the experimental source water used. Underprediction and overprediction of iron scale release occurred with source waters with extreme values for

sulfates, chloride, and/or alkalinity, extreme low temperatures, and for Reynolds values near stagnant flow. (Mutoti, Dietz et al. 2007b)

The application of the combined statistical and flux model into a typical water distribution model would require inputs from the flow model for determining hydraulic retention time, pipe material, and pipe diameter. To obtain an accurate flux term though, water chemistry parameters would need to be tested regularly. An accurate flux term determination is essential to make any useful calculations. A summary of the model parameters are seen below in Table 6.

Table 6 Summary of Data Requirements for Combined Statistical and Iron Release Flux Model

Model Parameter		Likely Data Source/ Method
Pipe Material	-	WDS CAD/GIS
Pipe Geometry	-	WDS CAD/GIS
HRT	-	Flow Model
Re Number	-	Flow Model
Chloride	-	Ion Chromatography
Sulfate	-	Ion Chromatography
Sodium Ion	-	Ion Chromatography / SCADA
DO	-	SCADA System
Temperature	-	SCADA System
Alkalinity	-	Endpoint Titration

3.3 Prediction of Discoloration in Distribution Systems Model (PODDS)

The PODDS model has been developed by J.B. Boxall, P.J. Skipworth, A.J. Saul, and others at the University of Sheffield in the UK. This model simulates particle mobilization and transport within the distribution system and attempts to predict the occurrence of discoloration events. Discoloration events are implied to be the directly related to suspended particulate. Particle settling is neglected based on the assumption that once

particles become resuspended/mobilized in the network, they are unlikely to re-deposit back onto the pipe surface. The model therefore incorporates the generation, development, and erosion of cohesive layers and other material on the pipe surface and the subsequent mobilization of and transport of these materials as permanently suspended in the bulk flow. (Boxall and Dewis 2005; Boxall and Saul 2005)

With this model, particle release from the pipe wall occurs as a result of hydraulic disequilibria inflicting forces beyond the particles ability to resist movement. Shear stress at the surface of the pipe wall can be calculated based on measured flow characteristics. Increases in shear stress (due to increases in flow) cause the release of corrosion products into the bulk flow of the pipe. This implies that the strength of the particle layer (ie. corrosion scale layer) is related to the typical flow regime within the pipe. Essentially, corrosion layers are conditioned by the typical daily flow patterns in the distribution network. When an increase in flow occurs beyond the typical pattern, stress is applied to the corrosion layers and a release event occurs. Additionally, it is assumed that the reservoir of particulate mass is also related to the typical flow pattern. A very weak particulate layer (ie. flow is typically very low) has a greater availability of particulate mass that a strong particulate layer (ie. high flows). With this model, turbidity serves as a surrogate for particulate mass (the model predicts changes in turbidity). Turbidity increases are assumed to be directly linked to corrosion scale and/or particulate release. Figure 9 below shows the relationship between the stored particulate mass (ie. stored turbidity volume) and the layer strength. (Boxall and Dewis 2005; Boxall and Saul 2005)

While flow inputs for this model could be derived from any typical water distribution modeling software, a number of the model variables must be determined

through a fairly extensive calibration procedure. Specifics of the model calculations and variables are seen below.

The shear stress term used for evaluating corrosion product release potential can be derived directly from the friction head loss term calculated using either the Darcy-Weisbach, Hazen-Williams, or Manning formulations for head loss due to friction. The strength of scaling on the pipe wall is assumed to be equal to the typical daily maximum shear stress value at the pipe wall and is related to the stored particulate volume (ie. stored turbidity volume) as follows. The stored turbidity volume is analogous to the thickness of the layer.

$$\tau_s = \frac{C^b - C_{max}}{k}$$

where,

τ_s = corrosion layer yield strength

C = measure of the turbidity potential of the layer

C_{max} = the upper limit for the stored turbidity of the layer

k = gradient describing the relationship between yield strength and the ability of the corrosion layer to increase turbidity

b = dimensionless power term

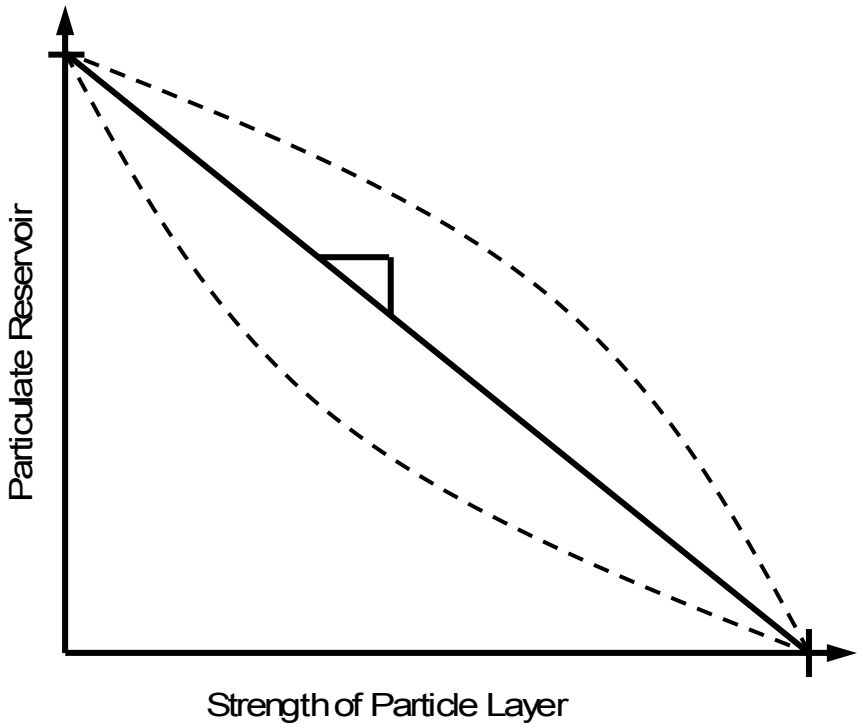

(Boxall and Saul 2005)

Figure 9 Turbidity potential versus layer strength

The release (ie. erosion) of the corrosion layer is defined as:

$$R_s = \frac{P(\tau_a - \tau_s)^n}{Q}$$

where,

R_s = the rate of supply from the corrosion layer

τ_a = the available shear stress at the pipe wall

Q = flow rate

P = dimensionless term

n = dimensionless term

Thus, the change in turbidity (ΔC_e) for a certain pipe segment is found by multiplying the supply rate (R_s) by the internal surface area (A_s).

$$\Delta C_e = R_s * A_s$$

To account for a discrete time step (Δt_{wq}), turbidity changes amount to:

$$\Delta C_e = R_s * Q * \Delta t_{wq}$$

The regeneration of the corrosion layer is primarily related to time and is thought to also be dependent upon temperature and layer conditions.

$$\Delta C_r = P' \Delta t T^l \tau_s{}^m$$

where,

ΔC_r = change in stored turbidity volume (due to regeneration)

P' = constant

Δt = change in time

T^l = effect of temperature

$\tau_s{}^m$ = effect of layer condition

For the above equations the variables P, P', n, b, k, τ_s, l, and m are problem dependent and require a calibration procedure to determine. This procedure would involve various flush tests and turbidity measurements. (Boxall and Saul 2005; Naser, Karney et al. 2006)

3.4 2-D Transient Multi-component Corrosion Model

This model was developed by G. Naser, B. W. Karney, and others at the University of Toronto's Department of Civil Engineering. Essentially, this model couples a 2-dimensional transient flow model with a 2-dimensional mass transport advection-diffusion-reaction equation (ADRE) for individual chemical species. This approach proposes a more realistic approach to simulation in three stated ways: consideration of reacting and interacting of chemical species, unsteady transient events, and cross sectional effects (Naser and Karney 2007). The coupling of these two components is accomplished by introducing two

numerical schemes. Specifically, the modified Vardy and Hwang approach developed by Zhao and Ghidaoui (2003) that utilizes the Method of Characteristics (MOC) is used to integrate the equations for flow hydraulics and a Finite Difference Method (FDM) is used to numerically integrate the ADRE. The FDM approach used is the Alternating Direction Implicit (ADI) approach. A standard five-region turbulence model is used to capture velocity fluctuations within a pipe section.

As mentioned above, the transient flow component is based on a modified Vardy and Hwang model. This model decouples the governing equations for flow into two sets of tridiagonal systems: one for piezometric head and radial flux and another for axial velocity (Zhao and Ghidaoui 2003; Naser and Karney 2007). The governing equations for 2-dimensional transient flow developed by Vardy and Hwang (Vardy and Hwang 1991) are as follows:

$$\frac{g}{a^2}\frac{\partial H}{\partial t} + \frac{\partial u}{\partial x} + \frac{1}{r}\frac{\partial rv}{\partial r} = 0$$

$$\frac{\partial u}{\partial t} + g\frac{\partial H}{\partial x} = \frac{1}{r\rho}\frac{\partial r\tau}{\partial r}$$

Where x is the distance along the pipe, r is the distance from the axis in radial direction, t is time, $H(x,t)$ is piezometric head, $u(x,r,t)$ is the local longitudinal velocity, $v(x,r,t)$ is the local radial velocity, g is gravitational acceleration, a is the wave speed, ρ is density, and τ is shear stress. The shear stress term (τ) is given by:

$$\tau = \rho\nu\frac{\partial u}{\partial r} - \rho\overline{u'v'}$$

Where ν is the kinematic viscosity and u' and v' are turbulence fluctuations corresponding to longitudinal velocity (u) and radial velocity (v) respectively. The term

$-\rho\overline{u'v'}$ can be defined by the five region turbulence model for pipes. More details on the algebraic derivation for the modified Vardy Hwang scheme can be found in (Zhao and Ghidaoui 2003).

The mass transport included is a second-order parabolic partial differential equation in cylindrical coordinate system for the *k*th chemical concentration:

$$\frac{\partial C_k}{\partial t} + U\frac{\partial C_k}{\partial x} + V\frac{\partial C_k}{\partial r} = \frac{1}{r}\frac{\partial}{\partial r}\left(rJ_{r_k}\right) + \frac{\partial J_{x_k}}{\partial x} \pm S(C_k)$$

Where *r* and *x* are coordinates in the cylindrical system, *U* and V are longitudinal and radial velocity components (respectively), *C* is the chemical concentration of *k* at point (x,r) and time *t*, J_x and J_r are the mass flux in the longitudinal and radial directions (respectively), *S(C)* is the source/sink term defining the generation or consumption of the *k*th chemical species. The ADI approach allows for numerical integration via two half steps. In the first step, the implicit is in the radial direction (denoted by *j*) and the explicit is in the longitudinal direction (denoted by *i*):

$$A_{k_1}C_{k_{i,j+1}}^{n+1/2} + B_{k_1}C_{k_{i,j}}^{n+1/2} + E_{k_1}C_{k_{i,j-1}}^{n+1/2} = F_{k_1}$$

In the second step, the explicit is in the radial direction and the implicit is in the longitudinal direction:

$$A_{k_2}C_{k_{i+1,j}}^{n+1} + B_{k_2}C_{k_{i,j}}^{n+1} + E_{k_2}C_{k_{i-1,j}}^{n+1} = F_{k_2}$$

The source/sink term in the mass transport ADRE incorporates the inclusion of iron release from the internal surface of the pipe. The boundary condition for this term defines the amount of iron (or turbidity in some instances) that is released from the pipe wall. There are three variations from the literature for how this term is treated. It should be noted that the intent of this model is "not to thoroughly describe the corrosion

phenomenon from either a chemical or physical point of view" rather "the goal is to highlight key hydraulic and chemical interactions influencing WQ transformations" (Naser and Karney 2007). While the description of the "corrosion phenomenon" is integral to the discussion at hand, it is important to note that the task of accurately defining and quantifying the corrosion release mechanisms took a peripheral role to developing a sophisticated flow and mass transport simulation framework for this model. Regardless, the three variations for treating this boundary condition are discussed as follows:

- Primary Corrosion Reactions: Under this scheme, the source/sink boundary condition is directly related to the primary corrosion reactions at the pipe wall. The primary corrosion reactions are defined by:

  Half Reaction: $Fe_{(s)} \rightarrow Fe^{2+} + 2e^-$

  Half Reaction: $\frac{1}{2}O_2 + H_2O + 2e^- \rightarrow 2OH^-$

  Overall Reaction: $Fe_{(s)} + \frac{1}{2}O_2 + H_2O \rightarrow Fe^{2+} + 2OH^-$

  Thus, the oxidation of metallic iron resulting in the release of ferrous ions defines the source term in this scheme. With a known first order kinetic coefficient, the amount of ferrous ion generation can be estimated based on the source water DO concentration. (Naser and Karney 2007)

- Extended Chemical Reactions: In addition to the primary corrosion reaction, this scheme incorporates the formation of ferric ions, carbonate species, and ferrous solids. Specifically, ferric ion formation from ferrous is included, as well as siderite formation ($FeCO_{3(s)}$) and ferrous hydroxide ($Fe(OH)_{2(s)}$) formation (which depend on carbonate species).

  Ferric ion formation:

$$Fe^{2+} + \tfrac{1}{4}O_2 + H^+ \leftrightarrow Fe^{3+} + \tfrac{1}{2}H_2O$$

Carbonate System:

$$CO_{2(aq)} + H_2O \leftrightarrow H^+ + HCO_3^-$$

$$HCO_3^- \leftrightarrow CO_3^{2-} + H^+$$

Siderite and Ferrous Hydroxide Formation:

$$Fe^{2+} + CO_3^{2-} \leftrightarrow FeCO_{3(s)}$$

$$Fe^{2+} + 2OH^- \leftrightarrow Fe(OH)_{2(s)}$$

Source/sink terms for each of the chemical species considered above are included in the mass transport simulation. It should be noted that the inclusion of these species was implemented on a 1-dimensional version of multi-component corrosion model (Baral, Karney et al. 2006).

- Coupling with PODDS: This form of the model simply treats the boundary condition for the source/sink term at the pipe wall according to the PODDS approach described above. Instead of tracking kinetic and equilibrium pathways for chemical constituents, this approach models the generation of turbidity in the WDS. This presents a significant variation for how this model treats the source of red water/discoloration. Whereas the approaches that derive the source generation terms from corrosion reactions handle corrosion release solely as a function of chemical reaction of water quality constituents, this approach treats the source for corrosion release as the erosion and suspension of corrosion materials at the pipe wall due to hydraulic (shear) forces. The erosion and suspension of corrosion materials is directly correlated to increases in turbidity. This model allows for a more robust shear stress determination as an input for the PODDS turbidity

simulation and in turn the turbidity simulation then serves as the input source/sink term for the mass transport ADRE. (Naser, Karney et al. 2006)

3.5 Resuspension Potential Method (RPM)

The Resuspension Potential Method has been developed by researches from Kiwa in the Netherlands. The RPM was created to aide in decision support and prioritization for network cleaning programs. While the RPM is not intended to be a computer model, it does provide a quantifiable indication for the risk of discoloration due to particle disturbance for a particular pipe segment. (Slaats, AwwaRF et al. 2003; Vreeburg, Schaap et al. 2004; Verberk, Doolan et al. 2007; Vreeburg 2007)

The RPM assumes that discoloration events are the direct result of particulate resuspension caused by disruptions in the hydraulic regime and that the source for particulate in the network may vary. The method involves isolating a section of pipe and applying a moderate increase in flow velocity of 0.35 m/s for fifteen minutes. The increase in flow velocity is in addition to the initial flow velocity that is observed in the pipe. During the test period, turbidity is continuously monitored for the water exiting the pipe. The turbidity response from the increase in flow typically contains four regions: the base turbidity level, the initial increase in turbidity at the start of the hydraulic disturbance, development of turbidity during the hydraulic disturbance, and resettling to base turbidity level. Figure 10 shows a typical turbidity response curve with the four regions. (Vreeburg, Schaap et al. 2004; Vreeburg 2007)

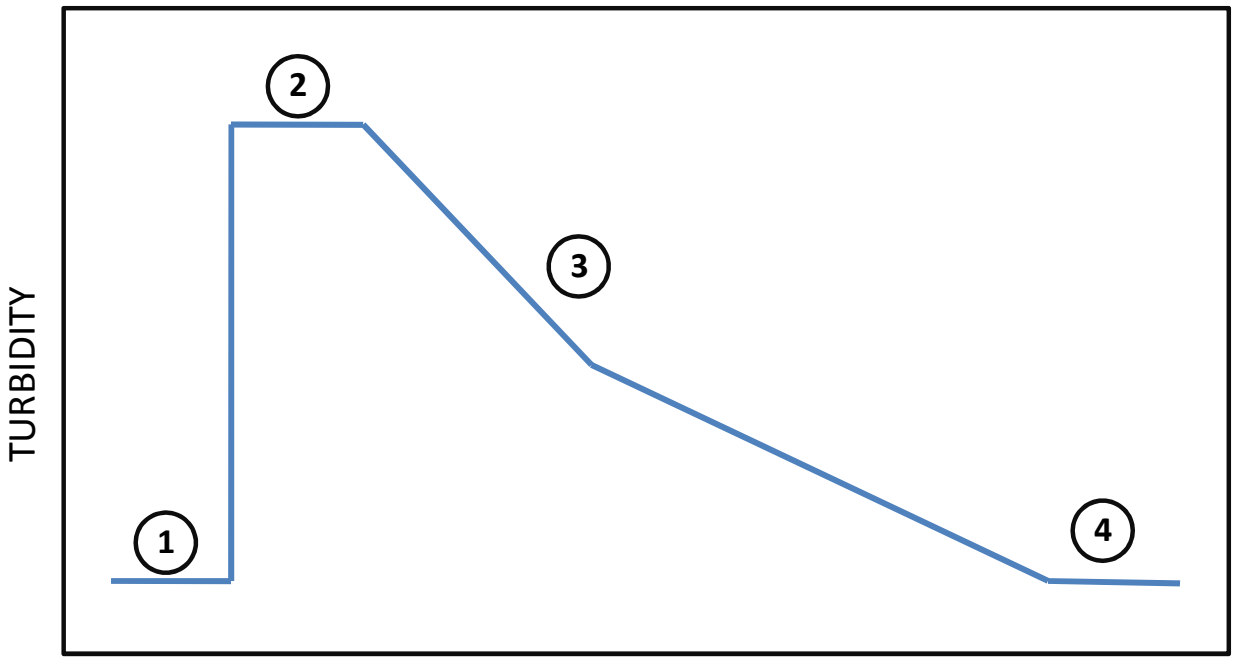

1 – Base turbidity level
2 – Initial increase in turbidity due to hydraulic disturbance
3 – Development of turbidity during hydraulic disturbance
4 – Resettling to base turbidity level

_____
(Vreeburg 2007)

Figure 10 Typical RPM turbidity response curve

The RPM method incorporates a rating system that ranks discoloration risk based on five aspects (all weighted equally). For each aspect, a ranking from 0 to 3 is made; 0 being the lowest risk, 3 being the highest risk. The five aspects that are ranked include:

- Absolute maximum value of turbidity during first five minutes of disturbance
- Average value of turbidity during first five minutes of disturbance
- Absolute maximum value of turbidity during last ten minutes of disturbance
- Average value of turbidity during last ten minutes of disturbance
- Time needed to resettle again to initial turbidity level

Table 7 and Table 8 below reveal example ranking categories for discoloration risk depending on the type of turbidity measuring equipment used. The rating scale for each RPM test must be calibrated to the specific turbidity equipment used and site specific considerations may be taken into account. A total score of 0 indicates that there is no resuspension potential for a pipe segment. The highest score is 15, indicating a maximum discoloration risk. This ranking system makes it easy to distinguish risks for discoloration in a WDS and can be used to prioritize approaches for network cleaning operations.

Table 7 RPM discoloration risk ranking table using the Sigrist KT65 equipment

RPM Aspect	Units	Score 0	1	2	3
Absolute max first 5 min	FTU	<0.3	0.3 - 1.0	1.0 - 2.4	> 2.4
Average first 5 min	FTU	<0.3	0.3 - 1.0	1.0 - 2.4	> 2.4
Absolute max last 10 min	FTU	<0.3	0.3 - 1.0	1.0 - 2.4	> 2.4
Average last 10 min	FTU	<0.3	0.3 - 1.0	1.0 - 2.4	> 2.4
Time to clear	min	< 5	5 - 15	15 - 60	> 60

(Vreeburg 2007)

Table 8 RPM discoloration risk ranking table using the Dr. Lange Ultraturb equipment

RPM Aspect	Units	Score 0	1	2	3
Absolute max first 5 min	FTU	<3	3 - 10	10 - 40	> 40
Average first 5 min	FTU	<3	4 - 10	11 - 40	> 40
Absolute max last 10 min	FTU	<3	5 - 10	12 - 40	> 40
Average last 10 min	FTU	<3	6 - 10	13 - 40	> 40
Time to clear	min	< 5	5 - 15	15 - 60	> 60

(Vreeburg 2007)

3.6 The Discoloration Risk Management (DRM) tool

The Discoloration Risk Management tool is being developed by Ewan Group PLC and Yorkshire Water Services in the UK. No readily available literature was discovered that details the DRM tool. Vreeburg and Boxall highlight the DRM tool in one of their papers

noting that the DRM is a risk based assessment tool that indicates the likelihood of pipe failure and discoloration. The risk assessment is based on 'expert panel' risk trees. Therefore the usefulness of the tool is limited by the knowledge and understanding used to develop the risk trees. (Vreeburg and Boxall 2007)

3.7 The Particle Sediment Model (PSM)

The Particle Sediment Model is being developed by the Corporate Research Centre in Australia. The PSM tracks transport, settling, and resuspension of particles in distribution systems. This model is not specific to iron scale release. It incorporates any particulate that may exist within the network that can contribute to discoloration. While the PSM model alone has no capabilities for predicting source quantities of discoloration materials (ie. iron or other particles), it can be used in conjunction with Time Integrated Large Volume Sampling (TILVS) equipment to measure sediment mass at various locations within the network and particle counters to observe changes in particle size and volume. (Jayaratne, Ryan et al. 2004; Verberk, Doolan et al. 2007)

The particle settling component of the PSM model is governed by the flow conditions. Under no flow (stagnant) conditions, settling is ultimately attributable to gravity and the rate of settling corresponds to the terminal velocity through water (terminal velocity is a function of particle size and specific gravity). Under laminar flow, particles are acted upon by Saffman and Magnus lift forces that can slow or maintain suspension of settling particles. During turbulent conditions (where Reynolds number is greater than 2,000), suspended particles are maintained in suspension and it is assumed that the mean vertical turbulent velocity is equal to or greater than the gravitational settling velocity. (Jayaratne, Ryan et al. 2004)

The resuspension component of the PSM model was initially developed using Shields curves for predicting entrainment of particles from a sediment bed. These curves allow for the prediction of particle resuspension when the shear stress at the bed is above a critical value. Table 9 below provides critical velocities required to resuspend particles for 100mm and 600mm diameter pipes. Note that critical velocities for resuspension depend not only on particle diameter, but pipe diameter as well. Also, it is important to note that the resuspension velocity is much greater than the velocity required to maintain an already suspended particle. (Jayaratne, Ryan et al. 2004)

Table 9 Velocity required for resuspension

Particle Diameter[1] (mm)	Velocity for Resuspension[2] (m/s)		Velocity for Resuspension (ft/s)[2]	
	100mm Pipe	600mm Pipe	4in Pipe	24in Pipe
0.200	0.220	0.275	0.722	0.902
0.100	0.195	0.250	0.640	0.820
0.050	0.186	0.190	0.610	0.623
0.020	0.125	0.160	0.410	0.525
0.010	0.090	0.120	0.295	0.394

[1] *Particle specific gravity = 2.6*

[2] *Pipe Roughness = 0.1mm*

(Jayaratne, Ryan et al. 2004).

Based on available literature and field and lab experiments, the three critical velocities associated with particle settling and resuspension have been estimated. These parameters are as follows:

- U_s: settling velocity of particles under no flow conditions
- U_d: velocity at which particles start to settle out of solution
- U_{rs}: velocity at which all particles are resuspended into solution

When flow velocity conditions are less than or equal to U_d, particles will settle out of solution. For flow velocities greater than U_d but less than or equal to U_{rs}, particles will be

maintained in suspension but no settled particles will be resuspended. When the flow velocity is greater than U_{rs}, all settled particles will be resuspended.

The transport function of the PSM tool essentially applies a mass balance on particulate matter to each pipe within a network of interest. Four mass parameters are calculated for each pipe over a time step with the PSM; these include: dM_{in}- particle mass transport into the pipe, dM_o- particle transport out of the pipe, M_x- particle mass per unit length along the pipe, M_s- particle mass settled. The PSM has been developed within a Windows platform and requires flow inputs from a calibrated hydraulic model as well as the particle setting velocities. (Jayaratne, Ryan et al. 2004)

4. Evaluation of Red Water Models

As discussed previously, red water events can be attributed to a wide range of sources dealing with hydraulic forces affecting the pipe, chemistry related interactions between the pipe and the delivered water, or other interactions. Each of the red water models developed typically emphasizes one of these aspects or variables that are thought to have an effect on red water problems. For example, the PSM tool emphasizes the hydraulic forces in the network as the primary source for red water. The statistical model, on the other hand, emphasizes water chemistry as the major factor in iron scale release. Additionally, the predictive emphasis of each model varies. While some of the models focus on predicting the release of iron scale, others emphasize the fate and transport of iron particles in the distribution system. The applicability of each model then, is dependent upon the specific circumstances with respect to a given water distribution system. This

chapter intends to highlight and evaluate where each of the aforementioned models may be most appropriately implemented.

4.1 Summary of Available Models

Table 10 below summarizes each of the models according to a number of parameters. The list below provides a brief explanation of each parameter considered.

- Predictive variable – this corresponds to the specific variable(s) that each model intends to predict.
- Scale release mechanism/red water source – this parameter indicates the primary driver for red water generation in each model. Generally, each model either assumes that red water is caused either by water chemistry factors or by hydraulic conditions.
- Scale formation component – A comprehensive red water model would ideally include a component to model the formation of iron corrosion layers. This component would allow for a more accurate estimation of the amount of source material available for release into bulk water. The PODDS model is the only model that comes close to including such a component. PODDS relates the amount of material available for red water generation to the typical daily flow velocity. A slower daily flow velocity corresponds to a weaker, more porous scale structure and therefore a greater amount of source material available for red water generation when flow is increased. A higher daily flow velocity corresponds to more structurally sound scale layers and therefore less source material is available when flow is increased. The 2-D Transient Corrosion model

that utilizes the corrosion reaction approaches does not consider scale layers as contributing to red water. This model identifies the initial corrosion reaction between water and metallic pipe as the source for red water.

- Pipe material – identifies whether the model is specific to pipe material or not. The Statistical model and the Flux model provide for red water release from cast iron and galvanized pipe. The 2-D Transient Corrosion model that utilizes the corrosion reaction approaches allows for iron release from non-specified iron pipe. The other models assume that layers of corrosion (or other) particles exist on all pipes within a distribution system.
- Particulate reservoir – this indicates the assumed source of particles causing red water. The Statistical model, Flux model, and PODDS attribute particles causing red water directly to corrosion scale layers (or "cohesive" layers). Implicit in this proposition is that once particles causing red water become suspended in the bulk water, no settling of particles occurs. The PSM tool, on the other hand, considers the mass of settled particulate as the source for red water. This model does not include a component for predicting the source generation of red water causing particles (although it has been noted that Time Integrated Large Volume Sampling can be used to estimate sediment mass within the WDS).
- Reservoir quantity – This corresponds to the total amount of material available for release. Mass release in the Statistical model and the Flux model is treated solely as a function of water chemistry and hydraulic forces respectively. Mass flux will continue to occur as long as conditions favorable for scale release remain. At first glance, this seems to imply that there is an infinite source of

material available for release. Rather, it should be seen that this implies that the net rate of corrosion scale formation (mass) is always equal to or greater than the rate of scale release. On the other hand, the resuspension potential method (RPM) relates the amount of material available to the observed turbidity response curve. Turbidity response curves typically reveal in initial spike in turbidity when flow is increased. This initial spike tails off eventually even while increased flow in maintained. Thus, the amount of particulate made available does not remain constant without limit. The reservoir quantity in the PODDS model is directly related to the scale formation component mentioned above. The amount of material available for release is a function of daily flow conditions. As the PSM tool calculates a mass balance of particles across pipe sections in a distribution system, the amount of source material available corresponds to the particulate mass being transferred into a pipe section from the upstream pipe section. No component is included to allow for the release of new material from scale layers.

- Water quality inputs –identifies which water quality variables are considered in predicting the occurrence of red water.
- Hydraulic inputs –identifies the hydraulic variables that are considered in predicting the occurrence of red water.
- Implementation – this provides an indication of the procedures required to implement each model. The PODDS and RPM models both require various procedures to be conducted in the field. The inputs for the Flux model and the PSM tool could be obtained using an available water distribution model (such as

EPANet). The PSM tool would also require an input to estimate the iron mass source. Inputs for the Statistical model would require analytical testing to determine water chemistry parameters.

- Commercial availability – none of the models are commercially available at this point. Code for the PODDS model has been written for EPANet and has been made available upon request.

Table 10 Summary of available iron release models

Parameter	Statistical Model[1]	Flux Model[2]	PODDS[3]	2-D Transient Corrosion Model[4]		Resuspension Potential Method[5]	Particulate Sediment Model[6]
				Corrosion Reaction Approaches	*PODDS Approach*		
Predictive Variable	Magnitude of source water's affect on iron release	Increase in iron concentration due to iron scale release	Generation and erosion of "cohesive" particle layers	Inc. in dissolved iron conc. due to iron corrosion	Generation and erosion of "cohesive" particle layers	Risk category for particulate resuspension	Particle transport, settling, and resuspension
Scale Release Mechanism/Red Water Source	Water chemistry factors	Reynolds number, pipe material, and pipe geometry	Hydraulic disequilibria	Corrosion of metallic iron	Hydraulic disequilibria	Water velocity increase	Water velocity
Scale Formation Component	None	None	Related to typical daily flow patterns	None	Related to typical daily flow patterns	None	None[7]
Pipe Material	Cast iron, galvanized pipe	Cast Iron, galvanized pipe	Any material	Iron	Any material	Any material	Any material
Particulate Reservoir	Iron corrosion scale	Iron corrosion scale	"Cohesive" particle layers	Iron pipe	"Cohesive" particle layers	Sediment in a pipeline	Settled particulate
Reservoir Quantity	Not considered	Not considered	Conditioned by typical flow pattern	Not considered	Conditioned by typical flow pattern	Related to turbidity response curve	Not considered[8]
Water Quality Inputs	Cl^-, SO_4^{2-}, Na^+, DO, Temp, Alk	Incorporated using the statistical model	Incorporated via calibration procedure	DO, carbonate species	Incorporated via calibration procedure	Not applicable	Not applicable
Hydraulic Inputs	HRT	Re, HRT, pipe material, pipe geometry	Water velocity/pipe shear stress	Modified Vardy Hwang transient hydraulic model	Shear stress term from transient hydraulic model	Water velocity	Water velocity
Implementation	Requires water quality analysis	Requires determination of flow conditions	Extensive calibration procedure	Requires coupling of sophisticated flow and ADRE systems	Extensive calibration procedure	Requires field testing procedure	Requires water vel. and iron mass source estimations
Commercial Availability	None	None	Code available for EPANet upon request	None	None	None	Unknown

[1] See :Imran, S. A., J. D. Dietz, et al. (2005). "Red water release in drinking water distribution systems." Journal American Water Works Association 97(9): 93-100.

[2] See: Mutoti, G. (2003). A Novel Model for the Prediction of Iron Release in Drinking Water Distribution Pipe Networks Department of Civil and Environmental Engineering, University of Central Florida. Ph.D. Dissertation.

[3] See: Boxall, J. B. and A. J. Saul (2005). "Modeling Discoloration in Potable Water Distribution Systems." Journal of Environmental Engineering 131(5): 716-725.

[4] See:Naser, G. and B. W. Karney (2007). "A 2-D transient multicomponent simulation model: Application to pipe wall corrosion." Journal of Hydro-environment Research 1(1): 56-69. Also: Naser, G., B. W. Karney, et al. (2006). Red Water and Discoloration in a WDS: A Numerical Simulation, ASCE. Also: Baral, M. P., B. W. Karney, et al. (2006). An Extended 1-D Transient Corrosion Model Including Multi-Component Chemical Species. 8th Annual Water Distribution Systems Analysis Symposium, Cincinnati, Ohio, ASCE.

[5] See: Vreeburg, J. H. G., P. Schaap, et al. (2004). Measuring Discoloration Risk: Resuspension Potential Method. 2nd IWA Leading-Edge Conference on Water and Wastewater Treatment Technologies, IWA Publishing.

[6] See: Jayaratne, A., G. Ryan, et al. (2004). "MODELLING OF PARTICLES IN WATER SUPPLY SYSTEMS Tracking the transport of particles in water distribution systems." Water : official journal of the Australian Water and Wastewater Association. 31(8): 28-34.

[7] While the PSM tool does not incorporate a way to estimate formation of iron scale, it does consider the mass of settled particulate.

[8] The authors note that the PSM tool can be used in conjunction with Time Integrates Large Volume Sampleing (TILVS) to measure sediment mass within a distribution system.

4.2 Discussion of Model Applications

Each of the models discussed in the report vary significantly. One of the primary differences has to do with the specific prediction that the model intends to simulate. While there are slight discrepancies between each model, each tends to either predict the

degradation and subsequent release of corrosion scale layers or the potential for resuspension and maintained suspension of (corrosion) particles in the distribution system. The 2-D Transient Corrosion Model that utilizes the corrosion reaction approaches stands somewhat alone in that it predicts the rate of the initial corrosion reaction instead of the handling secondary corrosion materials (scale layers). Models that focus on the degradation and subsequent release of corrosion layers include the Statistical Model for red water release, the Iron Release Flux Model, and the Prediction of Discoloration in Distribution Systems (PODDS) model. Models that predict the potential for resuspension and maintained suspension of (corrosion) particles include the Resuspension Potential Method (RPM) and the Particulate Sediment Model (PSM).

Generally speaking, the models that predict the degradation and release of corrosion scale layers assume that layers of scale exist along the interior surface of pipes and certain forces act on these layers as water is transferred thought the pipe to deteriorate and/or erode the layers. These models attempt to predict the amount of source material generation occurs in a specific pipe reach. Once source material is released, by default, these models assume that corrosion scale particles remain in suspension permanently. It is disputed whether this is always the case though (Jayaratne, Ryan et al. 2004; Boxall and Saul 2005; Vreeburg 2007). Some argue that it is likely that particles settle out in dead end and stagnant locations of the distribution system.

Models that predict the potential for resuspension and maintained suspension of (corrosion) particles track the transport of particles that exist within a WDS. This category of model interprets inputs (such as an increase in flow velocity) to predict or provide indication of the fate of particles that exist in the network. It is important to note that the

difference in these categories is subtle, yet it is important to note these differences to highlight the varying assumptions for the causes of red or discolored water. The models that focus on the suspension and resuspension of particles do not necessarily specify the source of particulate matter in the distribution system. They also assume that particles are loosely held together and that particulate settling is a significant occurrence. On the other hand, the models that predict the degradation and release of corrosion scale layers identify the source of red and discolored water to be dominated by corrosion products. Additionally, these models treat particles as "cohesive" or solid layers. As these layers deteriorate, the particles released are maintained in suspension without limit (ie. no particle settling is accounted for).

While disagreement as to the specific mechanisms that are responsible for red and discolored water formation still exists, it is likely that the applicability of each model is very site specific. Pipe age and material, water quality factors, source water treatment operations, system hydraulics are just a few of the factors that may vary significantly from one WDS to another. At this stage, the implementation of any of the corrosion release models will necessitate careful investigation of the WDS and lengthy studies to determine accuracy.

Another variation between the models has to do with how each model treats the amount of mass available to generate red water. As mentioned above, the Statistical Model and the Flux Model inherently assume that the rate of scale growth is equal to or greater than the rate of scale release and therefore the amount of material available for release is not limited. The RPM treats source mass available for red water formation as limited to an initial spike in water velocity (the PODDS model treats corrosion scale release similarly).

At first glance, these methods appear to contradict one another. Does the release of red water causing materials occur continuously over time or do releases occur during discrete events when alterations are made to the flow regime?

Experimental results from the Flux Model experiments showed increases in turbidity along a 6 inch diameter by 90 ft length cast iron pipe to be 0.057 NTU when the flow exhibited a Reynolds number of 8260 (flow velocity of around 0.054 m/s). The example scale ranges for RPM tests show an increase in a minimal of 0.3 FTU warrant a risk for discoloration (after an increase in flow velocity of 0.35 m/s). Assuming that NTU (nephelometric turbidity units) are roughly equivalent to FTU (Formazin turbidity units), these ranges vary significantly. Additionally, it is important to note that pipes were flushed to remove any extraneous particles prior to turbidity measurements during Flux experiments. This points to an important discrepancy in modeling priorities. While the RPM may be a useful tool for predicting the risk that particles may have a tendency to settle in certain sections of pipe and be resuspended when water velocity increases, the flux model experiments show that continued mass release from corrosion scale may continue over time when flow conditions remain constant. The RPM focuses on moments of disequilibria while the flux model deals with steady state conditions. This reveals that these models do not contradict one another; rather it is very possible that they could complement each other. Under consistent flow conditions, the flux model can predict the mass flux due to iron scale degradation. When pipe flow increases, incorporating the RPM (or PODDS model) may be able to provide some indication as to the expected spike in particle resuspension.

Variation is also seen in how each model handles pipe material. It seems logical to conclude that iron release will only occur in iron pipes since plastic and lined iron pipes do not experience iron corrosion and scale formation. Mutoti, Dietz et al. (2007a) highlight a study that showed just this. In a 12 month study testing iron release characteristics for various pipe materials, the effluent iron concentrations from lined cast iron and PVC pipes was negligible. Pipes in this study were excavated from existing full-scale distribution systems.

Another recent study found that iron particulate layers were generated in a laboratory based plastic (HPPE) pipe system supplied with water that is fully compliant with UK regulatory standards (turbidity of 0.15 NTU and iron concentration of 0.03 mg/L). Water entering this system came from a local treatment plant that utilized iron coagulant. The small amount of iron entering this system that was solely from the source water was capable of generating a "cohesive" particulate layer on the pipe surface (Husband, Boxall et al. 2008). This indicates that red water or discolored water problems may not always be attributed to corrosion problems. This example serves to highlight the complexity of red and discolored water problems. More research investigating the processes that may or may not lead to the attachment of particles in the distribution systems that form these 'cohesive' layers on pipe walls is needed. This phenomenon may be the result of a number of factors such as source water quality, pipe material, etc. Again, this shows that the incorporation of any of the corrosion release models will necessitate careful investigation. No catch all solution exists at this point.

The uncertainty in the specific mechanism resulting in iron release and red water formation is also evident when evaluating each of the iron release models. Section 1.3

above notes that it is still uncertain as to whether iron scale release is primarily the result of water chemistry factors, pipe hydraulics, or a combination of both. Additionally, there exists disagreement as to the extent that iron release occurs from dissolution processes or from particulate/film release mechanisms. Table 10 above identifies the variation for how each model treats the mechanism for scale release. Note that each of the models that emphasize pipe hydraulics as the mechanism for iron release are not in agreement on how this mechanism functions. The PODDS model and the RPM method identify a change (increase) in flow velocity as the culprit for release. The Flux Model and the PSM tool relate iron release (or particulate fate) directly to the distinct flow velocity. Again, this highlights the complexity of iron corrosion release processes and shows the care that should be taken before implementing any of the discussed models.

In comparing each iron release model, it is very important to consider the mindset and perspective of the creators. There is significant variation in the locations where each of the models has been developed: the United States, the United Kingdom, Canada, the Netherlands, and Australia. There are drastic differences between the specific operational preferences, water quality standards, source water, treatment considerations, etc. depending on the country or location.

For example, in the U.S., the Surface Water Treatment Rule requires a maintained secondary disinfectant residual of 0.2 mg/L and a max disinfection residual concentration of 4 mg/L throughout the distribution system (USEPA 2006). This applies to all surface waters as well as groundwater under direct influence of surface water. In Canada, six out of seven provinces that responded to a recent survey require a minimum disinfectant residual which range from a measureable level to 0.5 mg/L and most provinces do not set a

maximum residual level. The province that does not require any residual concentration relies solely on groundwater for drinking water (CWWA 2009). Drinking water standards in Europe are set by the European Union for member states. While EU standards require that waters are free of pathogens (typically measured by *E. coli*), primary and secondary disinfection is not required for drinking water (USEPA 2006). Specifically, in Finland, no disinfectant residual is required. Spain and France require minimums of 1.0 and 0.5 mg/L respectively. In Germany, chloramines are prohibited and health officials set the goal of having no disinfectant residual in drinking water (except under exceptional circumstances). In the Netherlands, no disinfectant residual is required; rather, the focus is on making drinking water free of pathogens through multiple barrier approaches and reducing levels of assimilable organic carbon (AOC) (CWWA 2009).

Variation is also found when comparing regulations regarding maximum turbidity levels. In Canada, six provinces out of eight that responded to a recent survey have a regulated maximum turbidity level which range from 0.5 NTU to 5.0 NTU (CWWA 2009). In the U.S., the Enhanced Surface Water Treatment Rule requires that 95 percent of all monthly samples be below 0.3 NTU for conventional and direct systems and 1.0 NTU for slow sand and diatomaceous earth plants (USEPA 2008; CWWA 2009). In Australia, the current maximum turbidity guideline is set at 5.0 NTU, but will likely be lowered to 1.0 NTU in the near future. In Switzerland, the maximum level is set at <0.2 NTU at the treatment plant. The U.K. has set a maximum turbidity level of 1.0 NTU at the plant and 4.0 NTU at the tap. In the Netherlands, the maximum turbidity level is set at 4.0 NTU at the tap. More notably, both the U.K. and the Netherlands have regulations that prohibit abnormal increases in turbidity. (CWWA 2009)

Depending on water source, supply infrastructure, disinfection philosophy, regulatory environment, etc., treatment and distribution practices may vary significantly from one location to the next. Also, the use of chloramines as a disinfectant in the U.S. may be absent in other parts of the world, especially Europe. While the variation between each of the models discussed in this report is closely related to the uncertainties and disagreements regarding corrosion release processes and mechanisms, much of this variation may also be attributed to the fact that water treatment and distribution looks different around the globe.

4.3 EXAMPLE

The Statistical Model and the Flux Model were developed simultaneously to allow for a combined model that incorporates the effects of water chemistry and hydraulics on corrosion scale release. An example simulation is worked out below.

4.3.1 COMBINED STATISTICAL AND FLUX MODEL

The Statistical Model provides an indication of the effect of the influent water chemistry on iron scale release in the WDS. The model predicts the change in apparent color (ΔC) expected from an influent water source. Seven water quality parameters are included in the determination: chloride ion concentration (Cl^-), sulfate concentration (SO_4^{2-}), sodium concentration (Na^+), dissolved oxygen content (DO), temperature (T), hydraulic retention time (HRT), and alkalinity (Alk) (all chemical species in mg/L, HRT has units of days, and temperature is in ^oC).

$$\Delta C = \frac{[Cl^-]^{0.485} * [SO_4{}^{2-}]^{0.118} * [Na^+]^{0.561} * [DO]^{0.967} * T^{0.813} * HRT^{0.836}}{20.9411 * [Alk]^{0.912}}$$

Example results that calculated the change in apparent color for four source waters are found in Table 11 below. Water 1 is seen to have the most detrimental effect on iron scale release, while Water 2 has the least detrimental effect.

Table 11 Example results from statistical model determination

	Water Quality Parameter							
Source Water	[Cl-]	[S042-]	[Na+]	[DO]	T	[Alk]	HRT	**ΔC**
Water 1	38	66	31.3	7.5	20	148	5	**10.18**
Water 2	14	7	10	9	20	100	5	**4.33**
Water 3	15	28	10.5	10	12.5	75	5	**5.32**
Water 4	15	28	10.5	9	20	75	5	**7.04**

The results from the statistical model can be directly implemented into the Flux Model. The ΔC_2 term (calculated using the statistical model equation) can be directly correlated to the flux term (K_{m2}) needed for the flux calculation.

$\frac{K_{m_1}}{K_{m_2}} = \frac{\Delta C_1}{\Delta C_2}$, and therefore $K_{m_2} = K_{m_1}\frac{\Delta C_2}{\Delta C_1}$ (Mutoti 2003)

The initial values for change in apparent color (ΔC_1) and flux term (K_{m1}) were determined experimentally, where $\Delta C_1 = 9.34$ and K_{m1} is a function of the Reynolds number and pipe materials (see Table 5 above). Once the flux term (K_{m2}) is determined, the change in iron concentration across a pipe section is calculated using the flux equation:

$$\Delta[Fe] = \frac{4K_{m2}HRT}{D}$$

Where,

Δ[Fe] is the change in iron concentration in mg/m^3

HRT is the hydraulic retention time in days

D is the pipe diameter in meters

Figure 11 and Figure 12 show example results across a wide flow range for a 24 inch section of 100 meter cast iron and galvanized pipe.

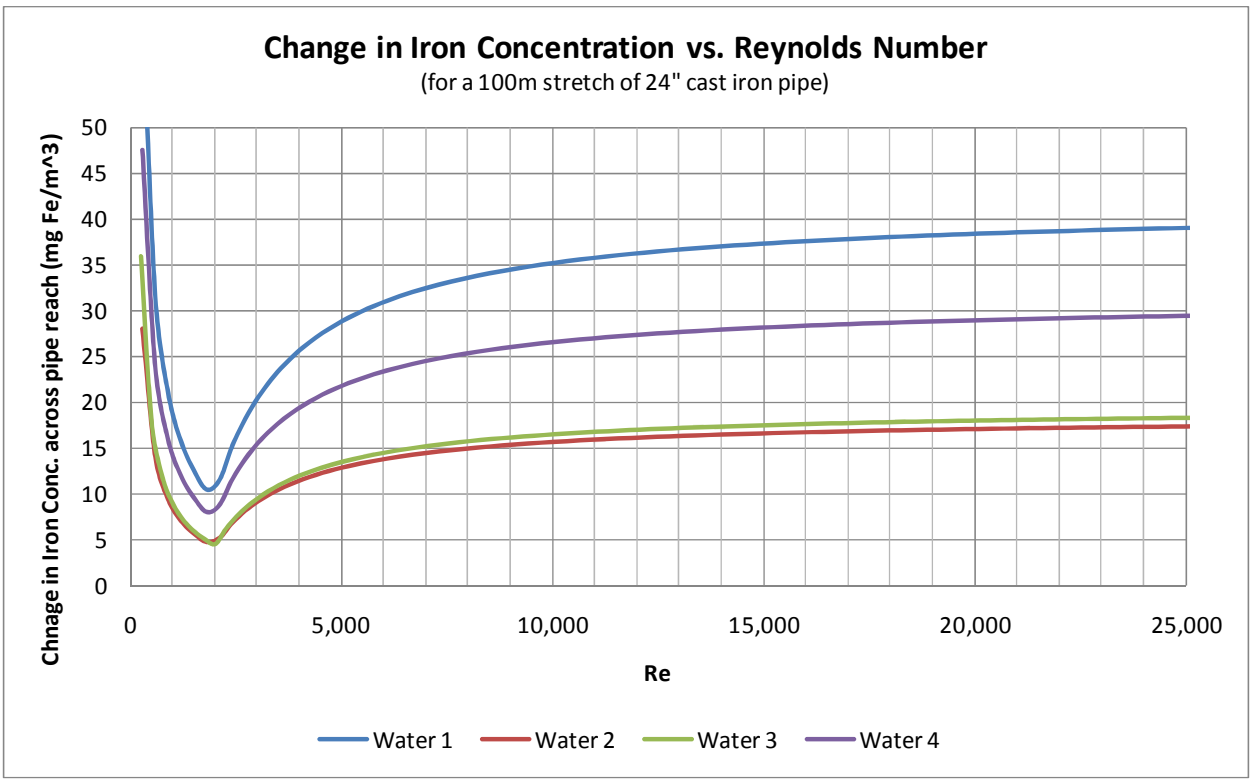

Figure 11 Example results for combined Statistical and Flux model for cast iron pipe

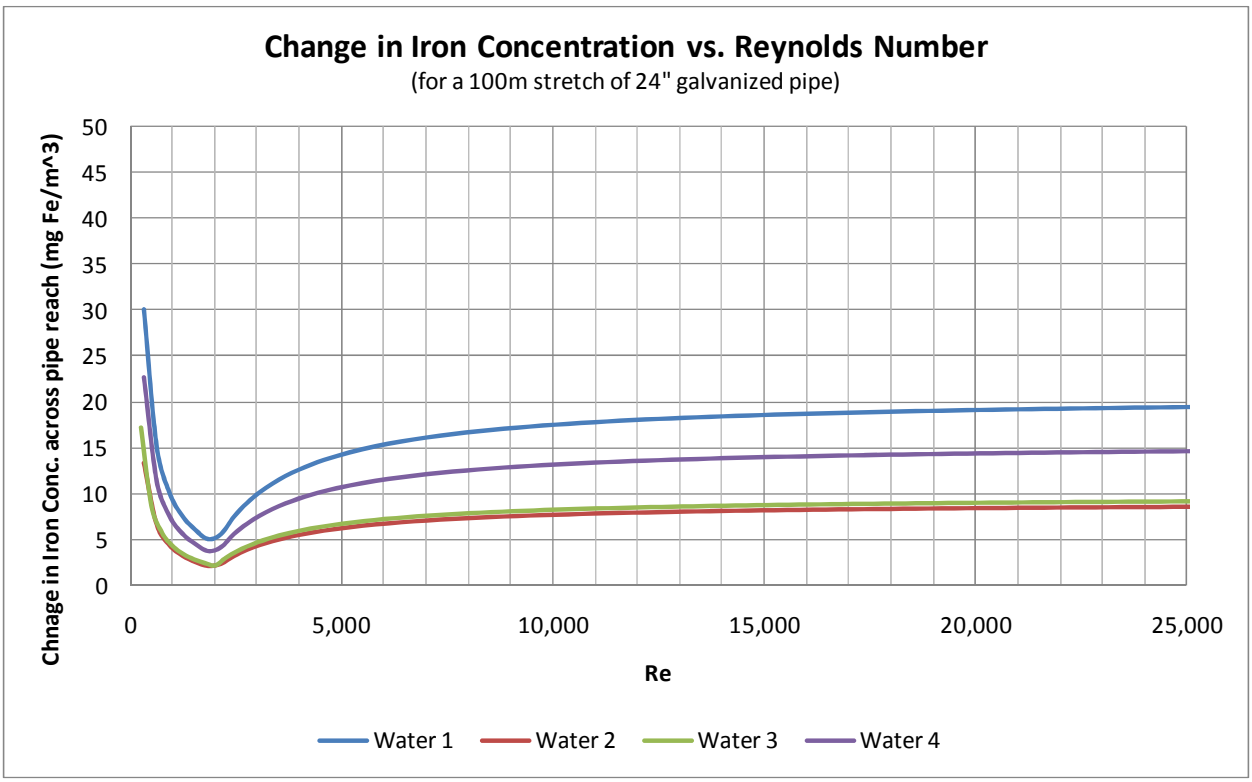

Figure 12 Example results for combined Statistical and Flux model for galvanized pipe

An example water distribution system was developed using EPANET in order to run a test simulation using the combined Statistical and Flux model. The WDS consists of a network of 500 ft cast iron pipes ranging from 4 inches to 12 inches in diameter. Demands are set at the nodes and the flow calculations (gpm) at 32 hours can be seen in Figure 13. The water source is a reservoir located in the upper left of the diagram. Arrows indicate flow direction. Pipe and node numbers are shown.

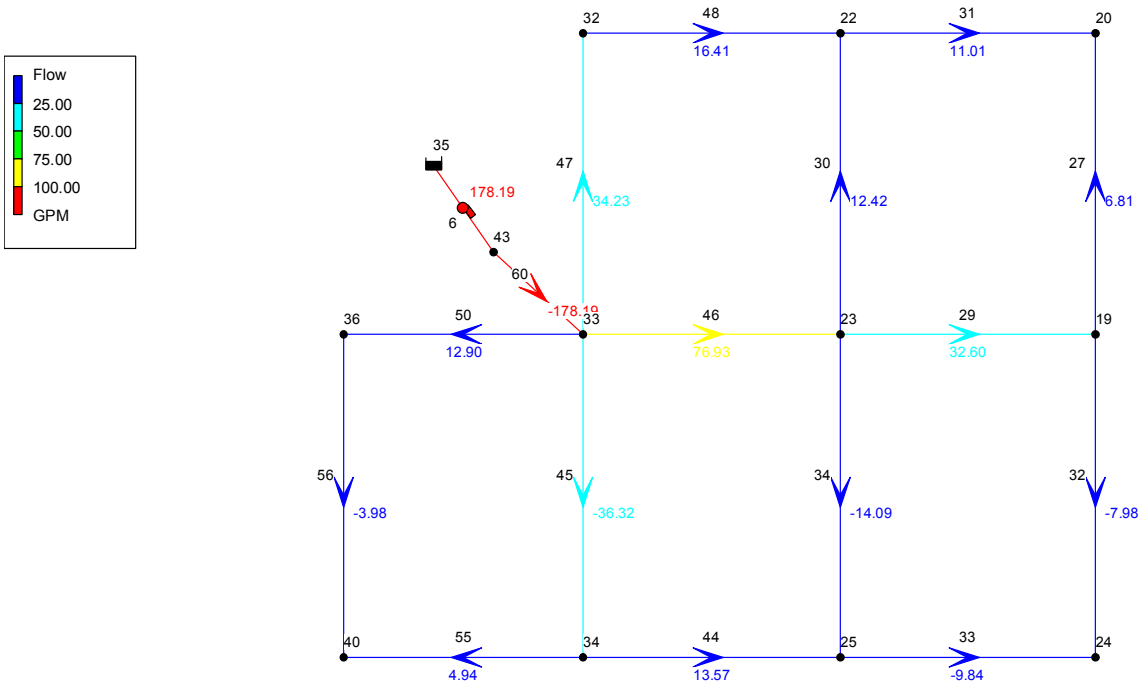

Figure 13 Example water distribution system in EPANET with flow calculations at 32 hours from start

Flow patterns were exported to MS Excel where flux calculations could be evaluated. The change in iron concentration across each pipe segment was calculated from the flux equation and the cumulative iron concentration was tracked at the nodes using the following mass balance equation:

$$C_{OUT} = \frac{\sum Q_{IN} C_{IN}}{\sum Q_{OUT}}$$

The influent iron concentration into a pipe was set equal to the concentration at the node directly upstream from the pipe. The total iron concentration in a pipe could therefore be obtained by summing the influent concentration and the change in concentration from the flux equation. A visual of the results of this exercise are seen in Figure 14. Note that total iron concentration is represented by the thickness of each pipe or node representation. As expected, the figure shows that as water moves through the WDS, total iron concentration gradually increases as water moves away from the source.

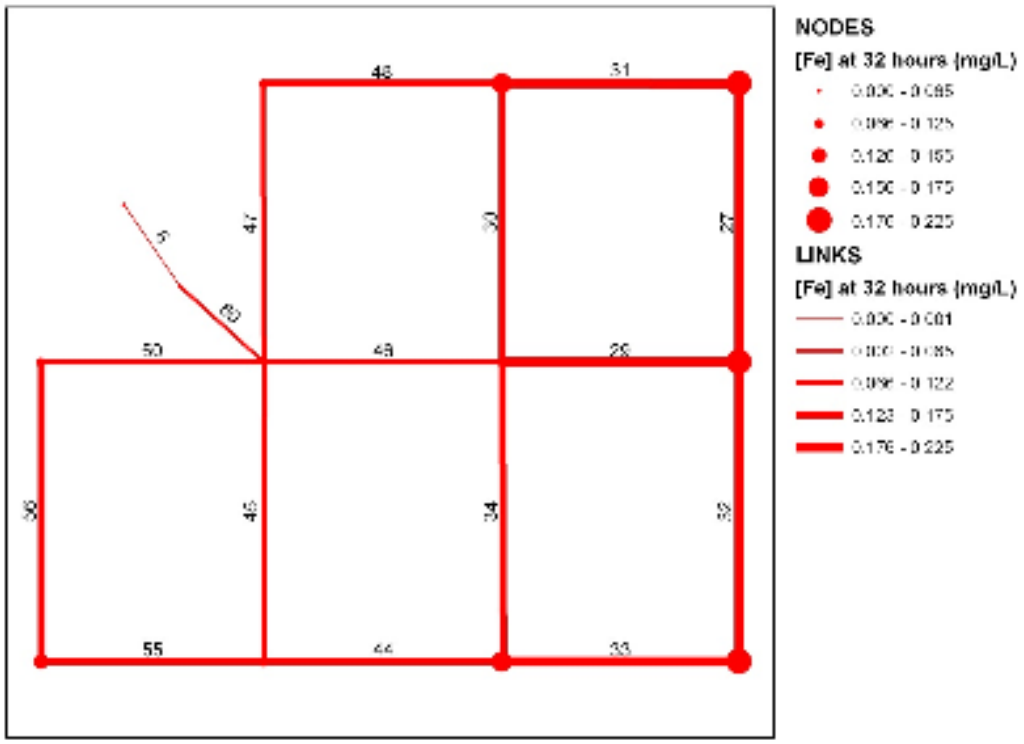

Figure 14 Visual results of the combined Statistical and Flux model example simulation

4.4 Conclusions

This report investigated available models for simulating iron corrosion release and red water events. This effort has led to the following conclusions:

- Numerous disagreements still exist as to the specific mechanism leading to iron scale release and red water formation. Disagreement or uncertainty exists as to:
    - The specific source of red and discolored water particles. It is still debated as to whether the source of particles in the distribution system is dominated by the deterioration of corrosion scale or if others sources should be taken into account.

    - The transport processes for particles in the distribution system. Specifically, the effect of particle settling in distribution systems is still debated.
    - Release mechanisms from corrosion scale layers.
    - Causes of corrosion scale deterioration. Scale layers may break down as the result of source water quality, hydraulic effects, some combination of both, or other factors.
    - Processes leading to the attachment of suspended particles to pipe wall and the subsequent formation of cohesive layers.
- These disagreements are highlighted is the variation of corrosion release models developed
- The variation of corrosion release models is also may also be influenced by the variation in water treatment and distribution practices around the world.
- Implementation of any corrosion release model will likely require detailed investigations into the characteristics of the WDS as well as lengthy studies testing the accuracy of the model

Appendix A Flux Model Derivation

The flux equation for the Iron Release Flux Model was derived both from the standard first order advection diffusion reaction equation (ADRE) as well as utilizing a mass balance with first order source generation (scale release) through a pipe section. Both derivations resulted in an identical flux equation. Derivations are seen below:

First order ADRE Equation minus diffusion:

$$\frac{\partial C}{\partial t} = \frac{-u\partial C}{\partial x} + k$$

Assume steady state, so $\frac{\partial C}{\partial t} = 0$,

Also: $\frac{\partial C}{\partial x} = \frac{dC}{dx}$, and

$$k = K_m * \frac{SA}{V}$$

So:

$$0 = \frac{-udC}{dx} + K_m * \frac{SA}{V}$$

Since $\partial x = u\partial t$, then

$$0 = \frac{-udC}{udt} + K_m * \frac{SA}{V}$$

$$\frac{dC}{dt} = K_m * \frac{SA}{V}$$

$$\Delta C = K_m * \frac{SA}{V} * \Delta t$$

$$\frac{SA}{V} = \frac{\pi DL}{\pi D^2 L/4} = \frac{4}{D}$$

$$\Delta t = HRT$$

$$\boldsymbol{\Delta C = \frac{4K_m HRT}{D}}$$

C = Concentration (M/L^3)
x = Location along pipe length
t = Time
u = Flow velocity (L/t)
k = Zero order rate constant ($M/L^3/t$)
SA = Surface area (L^2)
V = Volume (L^3)
K_m = Zero order mass flux term ($M/L^2/t$)
$\Delta t = HRT$ (Hydraulic Retention Time)

Mass Balance with first order generation:

Accumulation = Input – Output + Generation

$$0 = QC_{in} - QC_{out} + kV$$

$$kV = \left(K_m * \frac{SA}{V}\right) * V = K_m * SA$$

$$C_{out} - C_{in} = \Delta C = \frac{K_m * SA}{Q}$$

$$\frac{SA}{Q} = \frac{SA}{V/dt} = \frac{\pi DL}{\pi D^2 L/4 * dt} = \frac{4 * dt}{D} = \frac{4HRT}{D}$$

$$\boldsymbol{\Delta C = \frac{4K_m HRT}{D}}$$

Q = Volumetric flow rate (L^3/t)
C = Concentration (M/L^3)
k = Zero order rate constant ($M/L^3/t$)
V = Pipe volume (L^3)
SA = Surface area (L^2)
K_m = Zero order mass flux term ($M/L^2/t$)

BIBLIOGRAPHY

Ackers, J., M. Brandt, et al. (2001). Hydraulic characteristics of deposits and review of sediment modelling. Project 'Drinking Water Quality and Health - Distribution systems-DW/03', UK Water Industry Research, London, UK.

Al-Jasser, A. O. (2006). "Chlorine Decay in Drinking-Water Transmission and Distribution Systems: Pipe Service Age Effect." Water Research **41**: 387-397.

AwwaRF and D. V.-T. Wasser (1996). Internal corrosion of water distribution systems. Denver, CO, The Foundation.

Baral, M. P., B. W. Karney, et al. (2006). An Extended 1-D Transient Corrosion Model Including Multi-Component Chemical Species. 8th Annual Water Distribution Systems Analysis Symposium, Cincinnati, Ohio, ASCE.

Baylis, J. R. (1926). "Prevention of Corrosion and Red Water." Journal American Water Works Association **15**(6): 598.

Boxall, J. B. and N. Dewis (2005). Identification of Discolouration Risk through Simplified Modelling. 2005 World Water and Environmental Resources Congress, Anchorage, AK.

Boxall, J. B. and A. J. Saul (2005). "Modeling Discoloration in Potable Water Distribution Systems." Journal of Environmental Engineering **131**(5): 716-725.

Burlinkgame, G. A., D. A. Lytle, et al. (2006). "Why Red Water? Understanding Iron Release in Distribution Systems." Opflow - American Water Works Association(December 2006): 12-16.

Clement, J. A. (2002). Development of red water control strategies. Denver, CO, Awwa Research Foundation and American Water Works Association.

Cornell, R. M. and U. Schwertmann (1996). The iron oxides : structure, properties, reactions, occurrences, and uses. New York, VCH.

CWWA. (2009). "Drinking Water Disinfection and Turbidity Requirements - A Global Perspective." Retrieved May 5, 2009, from http://www.cwwa.ca/freepub_e.asp.

DiGiano, F. A. and W. D. Zhang (2005a). "Pipe section reactor to evaluate chlorine-wall reaction." Journal American Water Works Association **97**(1): 74-85.

Fan, L.-S. and C. Zhu (1998). Principles of gas-solid flows Cambridge, New York, Cambridge University Press.

Husband, P. S., J. B. Boxall, et al. (2008). "Laboratory studies investigating the processes leading to discolouration in water distribution networks." Water Research: doi:10.1016/j.watres.2008.07.026.

Imran, S. A., J. D. Dietz, et al. (2005). "Modified Larsons Ratio Incorporating Temperature, Water Age, and Electroneutrality Effects on Red Water Release." JOURNAL OF ENVIRONMENTAL ENGINEERING **131**(11): 1514-1520.

Imran, S. A., J. D. Dietz, et al. (2005). "Red water release in drinking water distribution systems." Journal American Water Works Association **97**(9): 93-100.

Jayaratne, A., G. Ryan, et al. (2004). "MODELLING OF PARTICLES IN WATER SUPPLY SYSTEMS Tracking the transport of particles in water distribution systems." Water : official journal of the Australian Water and Wastewater Association. **31**(8): 28-34.
Kirmeyer, G. J. (2000). Guidance manual for maintaining distribution system water quality. Denver, CO, AWWA Research Foundation and American Water Works Association.
Kirmeyer, G. J. and G. S. Logsdon (1983). "Principles of Internal Corrosion and Corrosion Monitoring." Journal of the Americal Water Works Association **75**(2): 78-83.
Langmuir, D. (1997). Aqueous Environmental Geochemistry, Prentice-Hall, Inc.
Mackey, E. D., H. Baribeau, et al. (2002). Public thresholds for chlorinous flavors in US tap water. 6th International Symposium on Off-Flavours in the Aquatic Environment, Barcelona, SPAIN, I W a Publishing.
McNeill, L. S. and M. Edwards (2000). "Phosphate Inhibitors and Red Water in Stagnant Iron Pipes." JOURNAL OF ENVIRONMENTAL ENGINEERING **126**(12): 1096-1102.
McNeill, L. S. and M. Edwards (2001). "Iron pipe corrosion in distribution systems." JOURNAL-AMERICAN WATER WORKS ASSOCIATION **93**: 88-100.
McNeill, L. S. and M. Edwards (2002). "The importance of temperature in assessing iron pipe corrosion in water distribution systems." Environmental monitoring and assessment **77**(3): 229-42.
Morton, S. C., Y. Zhang, et al. (2005). "Implications of nutrient release from iron metal for microbial regrowth in water distribution systems." Water Research **39**(13): 2883-2892.
Mutoti, G. (2003). A Novel Model for the Prediction of Iron Release in Drinking Water Distribution Pipe Networks Department of Civil and Environmental Engineering, University of Central Florida. **Ph.D. Dissertation**.
Mutoti, G., J. D. Dietz, et al. (2007a). "Development of a novel iron release flux model for distribution systems." Journal American Water Works Association **99**(1): 102-111.
Mutoti, G., J. D. Dietz, et al. (2007b). "Pilot-Scale Verification and Analysis of Iron Release Flux Model." Journal of Environmental Engineering **133**(2): 173-179.
Naser, G. and B. W. Karney (2007). "A 2-D transient multicomponent simulation model: Application to pipe wall corrosion." Journal of Hydro-environment Research **1**(1): 56-69.
Naser, G., B. W. Karney, et al. (2006). Red Water and Discoloration in a WDS: A Numerical Simulation, ASCE.
Piriou, P., E. Mackey, et al. (2002). Chlorinous flavor perception in drinking water. 6th International Symposium on Off-Flavours in the Aquatic Environment, Barcelona, SPAIN.
Rompre, A., M. Prevost, et al. (1999). Impacts of implementing a corrosion control strategy on biofilm growth. 4th International Conference on Biofilm Systems, New York, New York, I W a Publishing.
Sarin, P., J. A. Clement, et al. (2003). "Iron release from corroded unlined cast-iron pipe." Journal American Water Works Association **95**(11): 85-+.
Sarin, P., V. L. Snoeyink, et al. (2004). "Iron release from corroded iron pipes in drinking water distribution systems: effect of dissolved oxygen." Water Research **38**(5): 1259-1269.
Sarin, P., V. L. Snoeyink, et al. (2001). "Physico-chemical characteristics of corrosion scales in old iron pipes." Water Research **35**(12): 2961-2969.
Sarin, P., V. L. Snoeyink, et al. (2004). "Iron Corrosion Scales: Model for Scale Growth, Iron Release, and Colored Water Formation." Journal of Environmental Engineering **130**(4): 364-373.
Seth, A., R. Bachmann, et al. (2004). "Characterisation of materials causing discolouration in potable water systems." Water Science and Technology **49**(2): 27-32.

Shields, A. (1936). "Anwendung der Aehnlichkeitsmechanik und der Turbulenzforschung auf die Geschiebebewegung [Application of similarity principles and turbulence to bed-load movement]." Mitteilungen der Preussischen Versuchsanstalt fur Wasserbau und Schiffbau.
Shook, C. A. and M. C. Roco (1991). Slurry flow : principles and practice Boston, Butterworth-Heinemann.
Slaats, P. G. G., AwwaRF, et al. (2003). Processes involved in the generation of discolored water. Denver, CO, Awwa Research Foundation.
Subhasish, D. (1999). "Sediment threshold." Applied Mathematical Modelling **23**(5): 399-417.
USEPA (2006). The Effectiveness of Disinfectant Residuals in the Distribution System.
USEPA. (2008, June 5, 2008). "Drinking Water Contaminants." Retrieved November 12, 2008, from http://www.epa.gov/safewater/contaminants/index.html.
Vanoni, V. A. (1975). River Dynamics. Advances in applied mechanics, Academic Press**:** 2-81.
Vardy, A. E. and K. Hwang (1991). "A Characteristics Model of Transient Friction in Pipes." Journal of Hydraulic Research **29**(5): 669-684.
Verberk, J. Q. J. C., C. Doolan, et al. (2007). "International Collaborative Research on Discoloured Water: Identifying the causes of distribution system discolouration events." Water : official journal of the Australian Water and Wastewater Association. **34**(1): 144-149.
Vreeburg, J. H. G. (2007). Discolouration in drinking water systems: a particular approach, Technische Universiteit Delft. **Ph.D Dissertation:** 183.
Vreeburg, J. H. G. and J. B. Boxall (2007). "Discolouration in potable water distribution systems: A review." Water Research **41**(3): 519-529.
VREEBURG, J. H. G., P. SCHAAP, ET AL. (2004). MEASURING DISCOLORATION RISK: RESUSPENSION POTENTIAL METHOD. 2ND IWA LEADING-EDGE CONFERENCE ON WATER AND WASTEWATER TREATMENT TECHNOLOGIES, IWA PUBLISHING.
WRICKE, B., L. HENNING, ET AL. (2007). PARTICLES IN RELATION TO WATER QUALITY DETERIORATION AND PROBLEMS IN THE NETWORK, TECHNEAU D 5.5.1 + D 5.5.2.
ZHAO, M. AND M. S. GHIDAOUI (2003). "AN EFFICIENT SOLUTION FOR QUASI TWO-DIMENSIONAL WATER HAMMER PROBLEMS." JOURNAL OF HYDRAULIC ENGINEERING, ASCE **129**(10): 1007-1013.